

Reductions and Hydroborations

Addition of a hydrogen atom to a trigonal (sp^2) carbon atom is the theme of this chapter. Within this scope are additions of dihydrogen, hydrides, and hydroborations. For the latter, the product boranes may be converted to a number of useful functional groups, but this chemistry is not covered here (reviews: [1,2]). The chapter is divided into three parts: reduction of carbon-heteroatom double bonds, reduction of carbon-carbon double bonds, and hydroborations. Several books have been written on these topics, so the present coverage is necessarily selective. As in previous chapters, the coverage is intended to highlight particularly important and selective reagents, with an emphasis on understanding the factors that influence stereoselectivity.

7.1 Reduction of carbon-heteroatom double bonds

Larock's *Comprehensive Organic Transformations* lists over fifty reagents in the section "Asymmetric Reduction of Aldehydes and Ketones" [3]. The nonenzymatic entries can be divided into several categories based on reagent type and/or mechanism: lithium aluminum hydrides modified with chiral ligands, borohydrides modified (sometimes catalytically) with chiral ligands, chiral boranes that reduce carbonyls in a self-immolative chirality transfer process, and chiral transition metal complexes that catalyze hydrogenation or hydrosilylation. Each of these involves interligand asymmetric induction (Section 1.3). Only selected examples from each category will be presented in detail; the objective being to analyze the factors that determine enantioselectivity for each reaction. A judgement of which reducing agent is most selective and/or convenient depends on the substrate, but an attempt at a comprehensive evaluation of 10 ketone classes with available reducing agents was made a few years ago [4]. Highly selective reductions of the carbon-nitrogen bond have been achieved only recently. Examples of azomethine reduction are included in the following sections as appropriate.

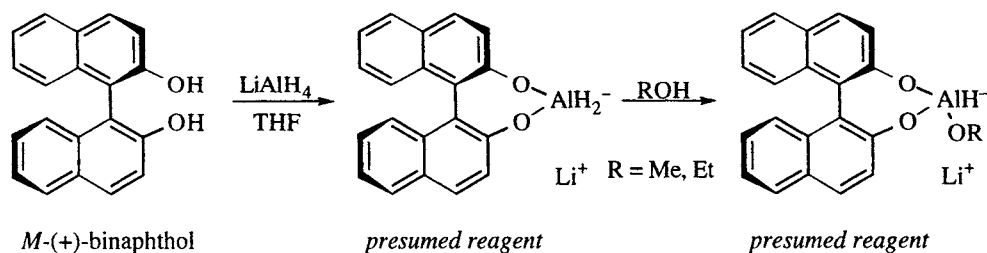
7.1.1 Modified lithium aluminum hydride

The first efforts to modify lithium aluminum hydride (LAH) with a chiral ligand were by Bothner-by in 1951 [5]. Although the result was later challenged, the seed was planted and many attempts have been made to produce an efficient chiral reducing agent using this strategy (reviews: [6-9]). Of these, we will examine the binaphthol-LAH-ROH reagent (BINAL-H) introduced by Noyori in 1979 [10-13]. Binaphthol is a popular ligand (like its cousin BINAP) for asymmetric synthesis because it has a pleasing C_2 symmetry which, when bound in a bidentate fashion to a metal, often affords excellent differentiation between heterotopic faces of a bound ligand.

Noyori's reagent is prepared by addition of binaphthol to a solution of LAH in THF, then adding another equivalent of an alcohol such as ethanol or methanol to form the reagent (Scheme 7.1).¹ The ethanol or methanol is a pragmatic necessity, as the reagent having two (presumed) active hydrides shows poor enantioselectivity in asymmetric reductions [12]. The exact nature of the reagent is not known, since aluminum hydrides may disproportionate and/or aggregate, processes that may continue as the product of the reduction (an alkoxide) accumulates during the reaction. Perhaps because of such processes, optimal selectivity is achieved with a 3-fold excess of the hydride reagent. Under these conditions, the reagent is highly enantioselective in reductions of certain classes of ketones. Some examples are listed in Table 7.1.

Entries 1 and 2 show the reagent's ability to reduce deuterated aldehydes to afford primary alcohols that are chiral by virtue of isotopic substitution. Note that the rest of the examples showing high selectivity (entry 13 being the exception) have one ketone substituent that is unsaturated and one that is not. Note also that in the saturated substituent, branching at the α -position lowers enantioselectivity significantly (compare entries 4/5 and 7/8). The fact that 3-octyn-2-one (entry 9) is reduced with 92% enantioselectivity (84% ee) whereas 2-octanone (entry 13) is reduced with only 62% enantioselectivity (24% ee) is curious. The authors submit that this comparison (among others) suggests that the facial discrimination involves more than just steric effects.

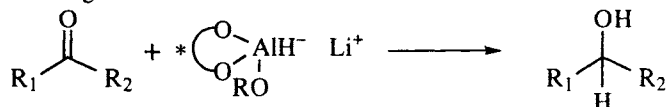
The rationale offered by the Noyori group to explain the chirality sense of the observed products is predicated on the 6-membered ring transition structures shown in Figure 7.1a and b. These structures differ only in the orientation of the two ketone substituents. Another pair, in which the 6-membered ring is flipped, is destabilized by a steric repulsion between the alkoxy methyl (or ethyl) and the C-3 position of the binaphthol. Figure 7.1c shows this interaction, which is (note the bold lines) a "gauche pentane-like" conformation (*cf.* Figure 5.5 and accompanying

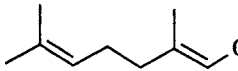
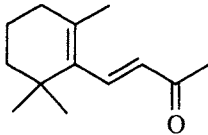


Scheme 7.1. Preparation of Noyori's BINAL-H reagents [12]. The aluminum complexes shown are postulated structures that may represent "time averages" of several equilibrating species.

¹ For those wishing to use this reagent, care should be taken to follow the Noyori experimental procedure exactly. Precipitous drops in enantioselectivity result from very minor changes in protocol. Note that a "milk-white" or "cloudy" reagent solution is OK; but when there is "extensive precipitation", the reagent should not be expected to perform as advertised [12] (see also ref. [14,15]).

Table 7.1. Asymmetric reductions using BINAL-H. The reactions were conducted by initial reaction at -100° for 3 hours, followed by several hours at -78° C. All examples favor *ul* relative topicity (see Figure 7.1a). Thus, the *M* reagent adds to the *Si* face to give the *R* product, and vice versa for the *P* reagent.



Entry	R ₁	R ₂	RO	% Yield	% es	Ref.
1	Ph	D	EtO	59	93	[13]
2			EtO	91	92	[13]
3	Ph	Me	EtO	61	97	[12]
4	Ph	<i>n</i> -Pr	EtO	92	100	[12]
5	Ph	<i>i</i> -Pr	EtO	68	85	[12]
6	α -tetralone		EtO	91	87	[12]
7	HC \equiv C	<i>n</i> -C ₅ H ₁₁	MeO	87	92	[13]
8	HC \equiv C	<i>i</i> -Pr	MeO	84	79	[13]
9	<i>n</i> -C ₄ H ₉ C \equiv C	Me	MeO	79	92	[13]
10	<i>n</i> -C ₄ H ₉ C \equiv C	<i>n</i> -C ₅ H ₁₁	MeO	85	95	[13]
11	<i>E</i> - <i>n</i> -C ₄ H ₉ CH=CH	Me	EtO	47	89	[13]
12	<i>E</i> - <i>n</i> -C ₄ H ₉ CH=CH	<i>n</i> -C ₅ H ₁₁	EtO	91	95	[13]
13	<i>n</i> -C ₆ H ₁₃	Me	EtO	67	62	[12]
14			EtO	87	100	[13]

discussion).² With respect to the 6-membered ring in Figures 7.1a and b, note that one of the ketone substituents is equatorial and one is axial. The interaction of the latter with the axial naphthyloxy ligand is postulated to account for the enantioselectivity. This interaction is suggested to be one of two types: steric interactions, which are repulsive, and electronic, which may (in principle) be either repulsive or attractive, but which are repulsive for all the examples in Table 7.1 (other substrates are suggested to have dominant *attractive* electronic interactions [12]). For the examples in Table 7.1, it is observed that the *P* BINAL-H reagent selectively adds hydride to the *Re* face (*ul* relative topicity - see Glossary, section 1.6), as shown in the transition structure of Figure 7.1a. In this structure, the saturated ligand (R_{sat}) bears a 1,3-diaxial relationship to the naphthoxy ligand on

² Note that in Figure 7.1a-c, the alkoxy "R group" is always axial. The authors point out that structures in which the R group occupies an equatorial position would be further destabilized by repulsive interactions between R and the BINOL moieties [12]. It may be useful to note that the configuration of the alkoxy oxygen in the favored chairs (Figure 7.1a,b) having the *P* BINOL ligand is *R*. The configuration of the oxygen in the disfavored chair (Figure 7.1c, *P* BINOL ligand) is *S*.

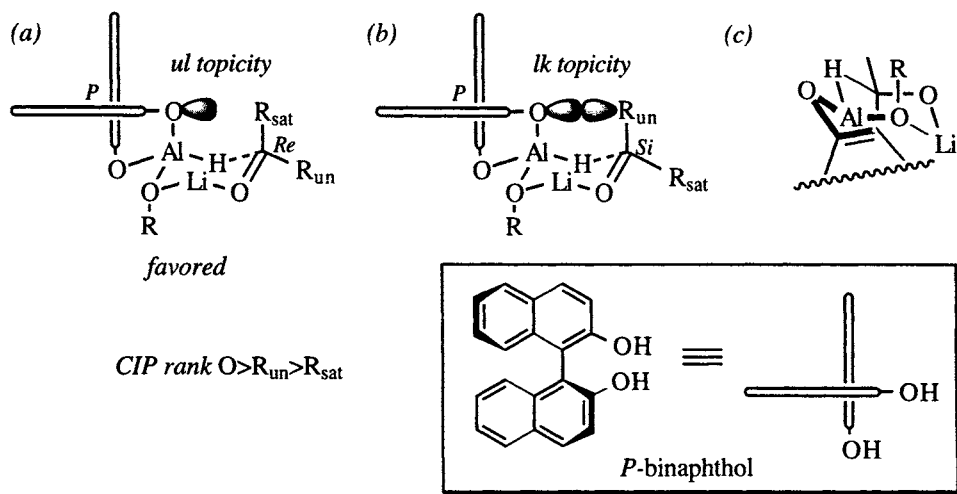


Figure 7.1. Postulated transition structures for the asymmetric reduction of unsaturated ketones by BINAL-H [12]. Structures (a) and (b) differ in the orientation of R_{sat} and R_{un} , the saturated and unsaturated ketone ligands, respectively. (a) *Ul* topicity: *P* reagent attacking *Re* face of ketone. (b) *Lk* topicity: *P* reagent attacking *Si* face of ketone. (c) Alternate chair that is destabilized by the "gauche pentane" conformation accentuated by the bold lines (cf. Figure 5.5). Transition structures containing this conformation were considered by Noyori to be unimportant [12].

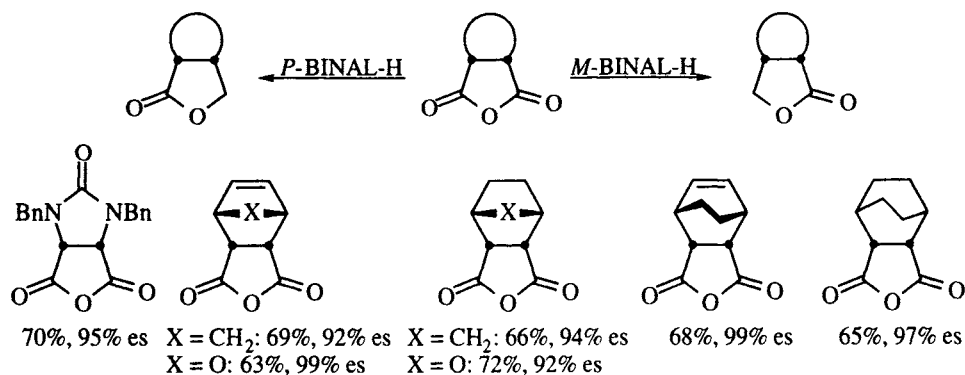
aluminum. Since an alkene or alkyne ligand is generally considered to be "smaller" than an *n*-alkyl ligand,³ this situation is somewhat counterintuitive. Noyori suggests that the reason for this topicity has to do with an unfavorable repulsive electronic interaction between the unpaired electrons on the axial naphthyl oxygen and the π orbital of the unsaturated ligand (R_{un}) in the transition structure having *lk* topicity, shown in Figure 7.1b, and that this interaction causes greater repulsion than that of an axial saturated ligand.

These reductions distinguish the enantiotopic *faces* of aldehydes and ketones. An interesting extension of the use of this reagent is the enantioselective reduction of *meso* anhydrides [17]. In this application, the reagent distinguishes enantiotopic *ligands*, not faces. A generic example of the process, along with yields and enantioselectivities of several substrates, is shown in Scheme 7.2.

7.1.2 Modified borane

The first attempt to use a chiral ligand to modify borane was Kagan's attempt at enantioselective reduction of acetophenone using amphetamine-borane and desoxyephedrine-borane in 1969 [18]. However, both reagents afforded 1-phenyl ethanol in <5% ee. The most successful borane-derived reagents are oxazaborolidines, introduced by Hirao in 1981, developed by Itsuno, and further developed by Corey several years later (reviews: [19,20]). Figure 7.2 illustrates several of the Hirao-Itsuno and Corey oxazaborolidines that have been evaluated to date. All of these examples are derived from amino acids by reduction or Grignard addition. Hirao

³ The *A* values of $-\text{CH}_2\text{CH}_3$, $-\text{CH}=\text{CH}_2$, and $-\text{C}\equiv\text{CH}$ are ~ 1.75 , 1.7 , and 0.41 kcal/mole, respectively [16].



Scheme 7.2. Yields and enantioselectivities of reduction of *meso* anhydrides using BINAL-H [17].

originally investigated the reagent derived from condensation of amino alcohols such as valinol and prolinol with borane (Figure 7.2a-c, e), and found enantioselectivities in the neighborhood of 70-80% es [21]. Optimization studies revealed that enantioselectivities of ~85% es (for the reduction of acetophenone) could be obtained in THF solvent at 30° C, using amino alcohol:borane ratios of 1:2 [22]. In 1983, Itsuno found that the reagent was much more selective (96-100% es with acetophenone) if tertiary alcohols derived from addition of phenyl magnesium bromide to valine (Figure 7.2d) were used [23,24]. Additionally, Itsuno found that a polymer-bound amino alcohol could be used for the process with equal facility [25]. Reduction of aliphatic ketones was not quite as selective, affording reduction products in 77-87% es [24,26]. Itsuno [24] and Corey [27] demonstrated the synthesis of oxiranes by asymmetric reduction of α -halo ketones followed by cyclization. In 1985, Itsuno showed that oxime ethers (but not oximes) could be enantioselectively reduced to primary amines (84-99% es) using the valinol-derived reagent (Figure 7.2d, [24]), and in 1987 showed that this process could be catalytic in oxazaborolidine: acetophenone *O*-methyloxime was reduced to α -methylbenzyl amine in 90% yield and 100% es [28]. In 1987, Corey characterized the Itsuno reagent (Figure 7.2d) and showed that the diphenyl derivative (Figure 7.2f) of the Hirao reagent (Figure 7.2e) afforded excellent enantioselectivities ($\geq 95\%$) when

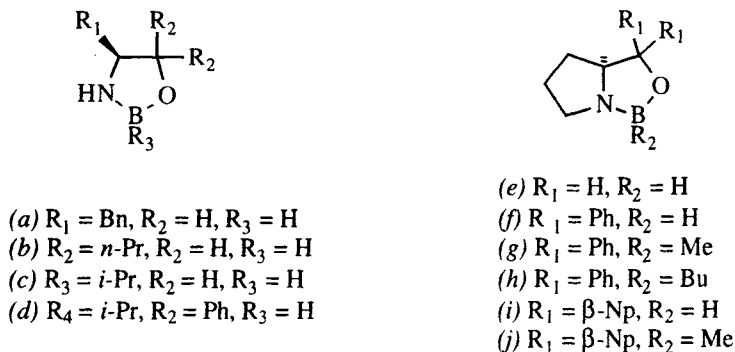
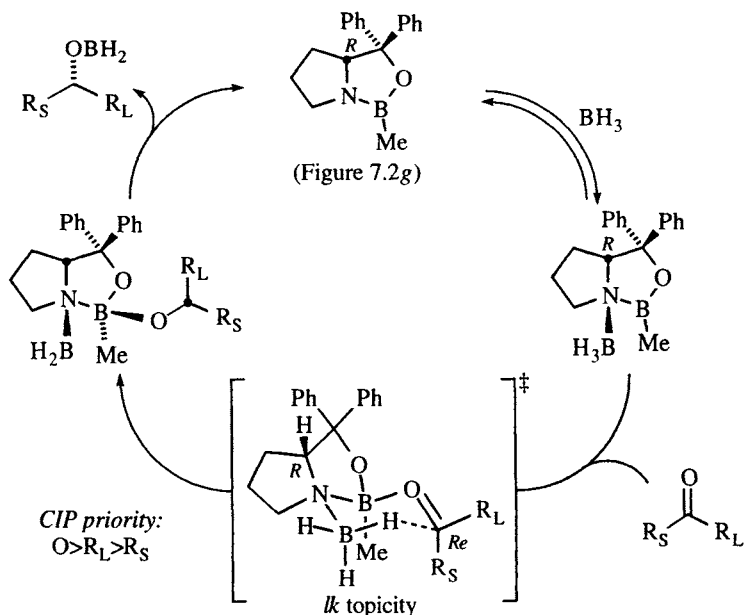


Figure 7.2. Oxazaborolidines for the asymmetric reduction of ketones: (a-c) [21,22]. (d) [23-26,28]. (e) [21]. (f) [29]. (g) [30]. (h) [27]. (i-j) [31].

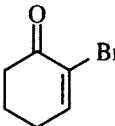
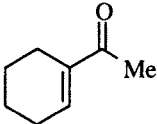
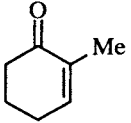
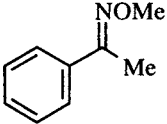
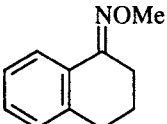
used in catalytic amounts [29]. In the same year, the Corey group reported that *B*-methyl oxazaborolidines (Figure 7.2g,h) were easier to prepare, could be stored at room temperature, could be weighed and transferred in air, and afforded enantioselectivities comparable to the *B*-H reagents [27,30]. In 1989, Corey found that the β -naphthyl derivative of prolinol afforded a reagent with still higher enantioselectivities than either the *B*-H (Figure 7.2i) or *B*-Me (Figure 7.2j) derivative (*e.g.*, 99% *es* with acetophenone [31]).

X-ray crystal structures of the oxazaborolidine reagent [32] and a derivative [33] have been published, and a mechanistic hypothesis has been formulated [29]. Heterocycles such as the boranes shown in Figure 7.2a-f,i do not, by themselves, reduce carbonyls; but in the presence of excess borane, they catalyze the reduction by the mechanism shown in Scheme 7.3 for the *B*-methyl catalyst of Figure 7.2g. In the first step, borane coordinates to the nitrogen of the oxazaborolidine on the less hindered convex face of the fused bicyclic system; the ketone then coordinates to the convex face. From the perspective of the ketone, the Lewis acid (boron atom) is *trans* to the larger ketone substituent [34]. Hydride transfer occurs *via* a 6-membered chair transition structure [35,36] having *lk* relative topicity (the *R* enantiomer of the catalyst favoring the *Re* face of the carbonyl carbon). Elimination of the alkoxy borane completes the catalytic cycle [37]. Table 7.2 lists representative examples of oxazaborolidine reductions. Entry 4 is one example (among several) of the asymmetric reduction [38] of trichloromethyl ketones [39]. Corey's group has shown that the resulting carbinols are versatile intermediates for the preparation of α -amino acids [38], α -hydroxy and α -aryloxy acids [40], and terminal epoxides [41].



Scheme 7.3. Catalytic cycle for the asymmetric reduction of a ketone with an oxazaborolidine catalyst [29,35,36].

Table 7.2. Examples of ketone reductions mediated by oxazaborolidines. The "Cat." column refers to the catalysts in Figure 7.2. The reductant is borane, unless otherwise noted. For entries 3 and 9, the product may spontaneously cyclize. The products of entries 16 and 17 are primary amines.

Entry	Ketone	Cat.	T, °C	% Yield	% es	Ref.
1	PhCOMe	<i>c, f-j</i>	2-30	95-100	≥97	[23,24,29-31,42]
2	PhCOEt	<i>c, f, g, j</i>	-10-30	100	≥94	[23,24,29-31]
3	PhCOCH ₂ Cl	<i>c, f, g</i>	25-32	100	98	[24,27,29,30]
4	<i>t</i> -BuCOCCl ₃	<i>h</i>	-20	96	99	[38]
5	α-tetralone	<i>f, g, i, j</i>	-10-31	100	≥93	[29-31]
6	<i>t</i> -BuCOMe	<i>f, g, j</i>	-10-25	100	≥96	[29-31]
7	<i>cyclo</i> -C ₆ H ₁₁ COMe	<i>g, j</i>	-10-0	100	91-92	[30,31]
8	<i>i</i> -PrCOMe	<i>c</i>	30	100	80	[24]
9	<i>n</i> -C ₆ H ₁₃ COMe	<i>c</i>	30	100	79	[24,26]
10	PhCO(CH ₂) _n CO ₂ Me n = 2, 3	<i>g, j</i>	0	100	97-98	[30,31]
11		<i>g, i</i>	23-36	100	95	[30,31]
12		<i>h</i>	-78 ^a	>95	90	[43]
13	<i>E</i> -PhCH=CHCOMe	<i>h</i>	-78 ^a	>95	96	[43]
15		<i>h</i>	-78 ^a	>95	96	[43]
16		<i>c</i>	30	90-100	99-100	[24,28]
17		<i>c</i>	30	100	84	[24]

^a Catechol borane as reductant

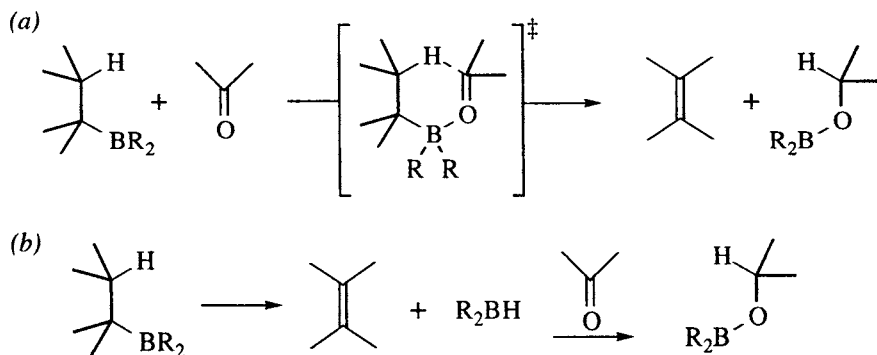
Operationally, these reagents are effective at or near room temperature, which may be of significant benefit to large-scale employment. The preparation of the *S*-diphenylprolinol ligand (*cf.* Figure 7.2*f-h*) is most easily accomplished by addition of a phenyl Grignard reagent to *L*-proline *N*-carboxyanhydride (73% yield, 99%

ee, [33]). The *R* enantiomer of the amino alcohol may be made by a similar addition to *D*-proline, but may also be made by enantioselective lithiation of BOC-pyrrolidine and addition to benzophenone (70% yield, 99% ee, as illustrated in Scheme 3.33 [44]).⁴ The catalysts may be made by condensation of the amino alcohol with methyl boronic acid [30,31,33] or trimethylboroxine [33] with simultaneous water removal. *B*-Methyl or *B*-butyl catalysts can be made by condensation of the amino alcohol with bis(trifluoroethyl) alkylboronate and removal of trifluoroethanol *in vacuo* [42].

The catalysts may be used in 5-10 mol% concentrations, with either borane or catechol borane [43] as the stoichiometric reductant. Use of the more reactive catechol borane allows one to conduct the reduction at lower temperature, a feature that may be advantageous in cases where selectivity at room temperature is not high enough. The reductions are sensitive to moisture: Jones, et al. [45] found that the presence of 1 mg of water per gram of ketone lowered the enantioselectivity from 97% to 75% es.

7.1.3 Chiral organoboranes⁵

The reaction of a chiral alkene with borane in the proper stoichiometry may afford alkyl boranes R^*BH_2 or dialkyl boranes R_2^*BH , where R^* is a chiral ligand. Attempts to achieve highly selective reductions of ketones using such reagents have met with little success, however.⁶ Trialkyl boranes R_3B were first reported to reduce aldehydes and ketones (under forcing conditions) in 1966 by Mikhailov [50]. Mechanistic studies (summarized in ref. [46]) showed that there are two limiting mechanisms for the reduction of a carbonyl compound by a trialkylborane, as shown in Scheme 7.4: a pericyclic process reminiscent of the Meerwein-Ponndorf-Verley reaction (Scheme 7.4a), and a two step process that involves dehydro-



Scheme 7.4. Limiting mechanisms for carbonyl reduction of carbonyls by a trialkylborane: (a) pericyclic mechanism. (b) Two step mechanism involving dehydroboration of a trialkylborane followed by carbonyl reduction by the resultant dialkylborane.

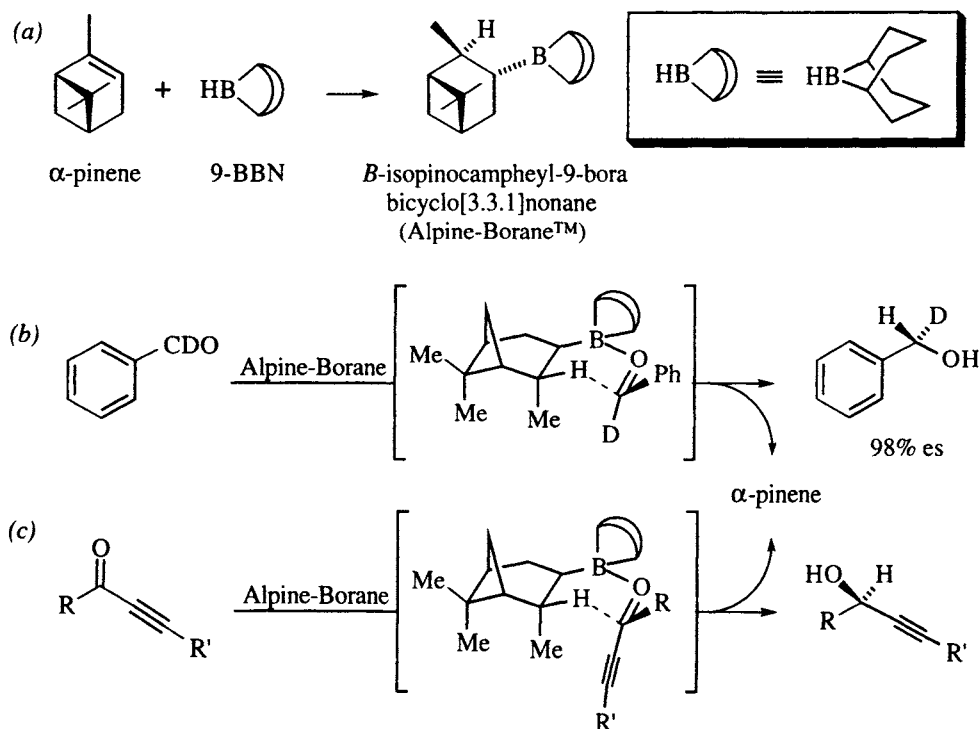
⁴ This procedure will be published in *Organic Syntheses*, probably in volume 74, 1996 (P. Beak, personal communication).

⁵ Reviews: ref. [46-48].

⁶ For a notable exception, see ref. [49].

boration to a dialkylborane plus olefin, followed by carbonyl reduction by the dialkylborane (Scheme 7.4b). With unhindered carbonyl compounds such as aldehydes, the reaction is bimolecular and appears to proceed by the pericyclic pathway [51]. With ketones, the rate is independent of ketone concentration, indicating a switch to the dehydroboration-reduction pathway.

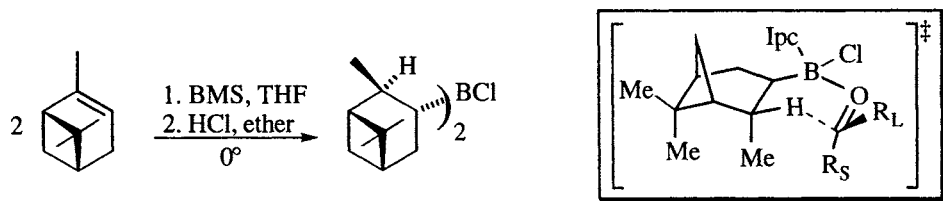
In 1979-80, Midland showed that the trialkyl borane formed by hydroboration of α -pinene by 9-borabicyclononane (9-BBN), known as *B*-isopinocampheyl-9-borabicyclo[3.3.1]nonane or Alpine-boraneTM, efficiently reduces aldehydes [52,53] and propargyl ketones [54,55] with a high degree of enantioselectivity, as shown in Scheme 7.5. The mechanism was shown to be a self-immolative chirality transfer process (Scheme 7.4a), proceeding through the 6-membered ring boat transition state shown in Scheme 7.5b and c [46]. This reduction is probably the method of choice for the production of enantiomerically enriched primary alcohols that are chiral by virtue of isotopic substitution, provided enantiopure α -pinene is used [56]. Most ketones other than propargyl ketones are not readily reduced by trialkylboranes, making this process highly chemoselective for aldehydes and propargyl ketones in the presence of other ketones, esters, acid chlorides, alkyl halides, alkenes and alkynes. Under forcing conditions, Alpine-borane dehydroborates (the reverse of Scheme 7.5a) with a half-life 500 min in refluxing THF [46], and non-selective reduction by 9-BBN becomes competitive (*cf.* Scheme 7.4b).



Scheme 7.5. Alpine-borane method of asymmetric reduction. (a) Preparation of Alpine-BoraneTM. (b) Reduction of deuterio benzaldehyde [52]. (c) Reduction of propargyl ketones [54,55].

To circumvent the problem of competitive dehydroboration with ketones, the Alpine-borane reductions can be conducted in neat (excess) reagent [57] or at high pressure (6000 atm, [58]). Experiments done in neat reagent take several days to go to completion, and afford enantioselectivities of 70-98% [57]. At pressures of 6000 atmospheres, the reactions are faster and dehydroboration is completely suppressed. Ketones are reduced with slightly higher enantioselectivities (75-100% es) under these conditions [58].

A better solution to asymmetric ketone reduction is to make a more reactive borane. Brown showed that hindered dialkylchloroboranes (R_2BCl) are less prone to dehydroboration than hindered trialkylboranes (R_3B) such as Alpine-borane and are excellent reagents for the reduction of aldehydes and ketones. Inductive electron withdrawal by the chlorine also increases the Lewis acidity of the boron. *B*-Chlorodiisopinocampheylborane (Ipc_2Cl , DIP-chlorideTM) is such a reagent, and is an excellent reagent for the asymmetric reduction of aryl-alkyl ketones [59,60]. Scheme 7.6 shows the preparation of Ipc_2Cl and the postulated transition structure to rationalize the chirality sense of the products. Table 7.3 lists several examples. Note that dialkyl ketones and alkynyl-alkyl ketones are reduced with low selectivity unless one of the substituents is tertiary. For a summary of other pinene-based self-immolative reducing agents, see Brown's reviews [47,48].



Scheme 7.6. Preparation of Ipc_2Cl . *Inset:* Proposed transition structure for asymmetric reductions using Ipc_2Cl [59].

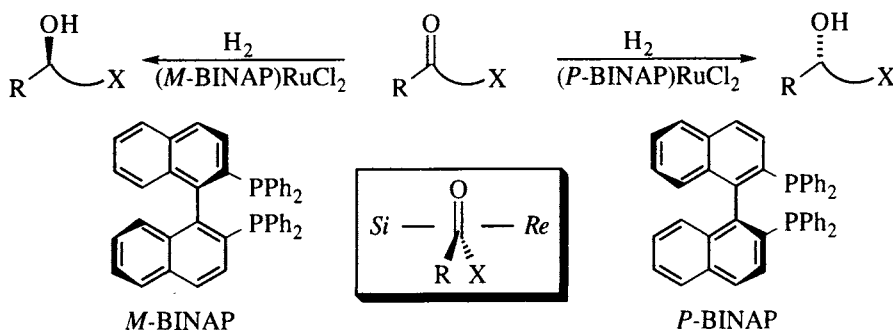
Table 7.3. Asymmetric reduction of ketones; $R_1C(=O)R_2$, with Ipc_2Cl .

Entry	R_1	R_2	% yield	% es	Ref.
1	Me	Et	—	52	[59]
2	Me	<i>i</i> -Pr	—	66	[59]
3	Me	<i>t</i> -Bu	50	93	[59]
4	2,2-dimethylcyclopentanone		71	98	[59]
5	2,2-dimethylcyclohexanone		60	91	[59]
6	1-indanone		62	97	[59]
7	α -tetralone		70	86	[59]
8	$HC\equiv C$	Me	83	58	[60]
9	$PhC\equiv C$	Me	92	60	[60]
10	$PhC\equiv C$	<i>i</i> -Pr	85	92	[60]
11	$PhC\equiv C$	<i>t</i> -Bu	80	>99	[60]
12	<i>cyclo</i> - $C_5H_{11}C\equiv C$	<i>i</i> -Pr	81	69	[60]
13	<i>cyclo</i> - $C_5H_{11}C\equiv C$	<i>t</i> -Bu	76	98	[60]
14	<i>n</i> - $C_8H_{17}C\equiv C$	<i>i</i> -Pr	86	63	[60]
15	<i>n</i> - $C_8H_{17}C\equiv C$	<i>t</i> -Bu	77	99	[60]

7.1.4 Chiral transition metal catalysts

Enantioselective reduction of simple ketone carbonyls is possible, but catalysts that deliver consistently high selectivities in such reactions have been elusive [61-64]. More success has been recorded in the asymmetric reduction of functionalized ketones and imines (reviews: [65,66]). Two types of stoichiometric reductants are used: dihydrogen and dihydrosilanes (reviews: ref. [67,68]), but as the mechanism of hydrosilylation is "highly controversial" [68], we will discuss only the former.

Ketone reductions. For the asymmetric hydrogenation of functionalized ketones, a team led by Noyori in Nagoya and Akutagawa in Tokyo introduced ruthenium(II) BINAP catalysts that produce excellent enantioselectivities for a number of functionalized ketones [69-75] (review: [76]; for a recent reference to a more reactive catalyst see ref. [77]). The topicity of the reduction is illustrated in Scheme 7.7, and is suggestive of a mechanism in which the heteroatom X and the carbonyl oxygen chelate the metal (*vide infra*). The catalyst is thought to be a monomeric BINAP ruthenium(II) dichloride, which was originally prepared by a tedious process using Schlenk techniques [69]; however, improved procedures have since been developed [71-73].

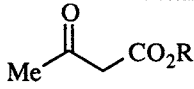
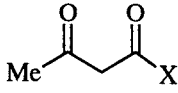
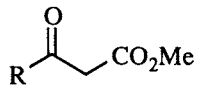
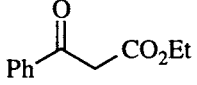
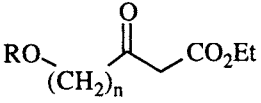
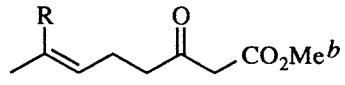
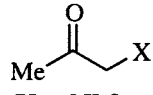
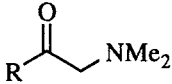


Scheme 7.7. *U*l relative topicity (e.g., *P*-BINAP/*Re* face) is uniformly observed for ruthenium BINAP catalyzed asymmetric reduction of functionalized ketones [70].

Selected examples that afford high selectivity are listed in Table 7.4. Several β -keto esters are reduced with excellent enantioselectivity (entries 1, 3-6); however, α -keto esters are reduced with somewhat diminished enantioselectivity [70]. β -Keto amides and thioesters (entry 2) are good substrates, as are α - and β -hydroxy ketones (entry 7) and α -amino ketones (entries 7 and 8). Particularly striking is the chemoselectivity observed when the reductions are conducted at low pressures: isolated double bonds are left intact (entry 6). Bifunctional ketones may be problematic, since chelation might occur by more than one functional group. For example, a ketone such as $\text{HOCH}_2\text{COCH}_2\text{CO}_2\text{Et}$ could chelate *via* either the hydroxyl or the ester oxygen, and this competition would lower the enantioselectivity. However, protection of hydroxyl as its triisopropylsilyl (TIPS) ether prevents chelation by the hydroxyl oxygen and excellent enantioselectivity results (entry 5). Competition is less of a worry if chelation forms a 6-membered ring, and protection as a benzyl ether suffices (entry 5).⁷

⁷ For an example of the effect of chelation on regioselectivity, see Scheme 4.3 and the accompanying discussion.

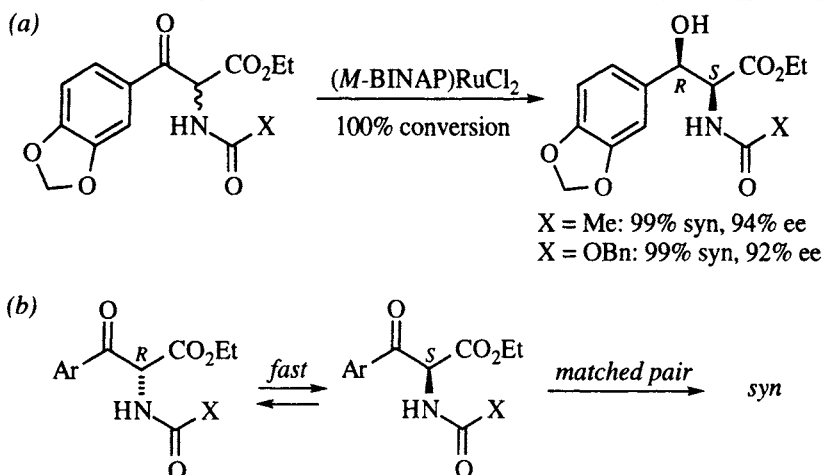
Table 7.4. Selected examples of asymmetric ketone reductions using $\text{Ru}^{\text{II}}\text{Cl}_2 \cdot \text{BINAP}$. Reactions were run at room temperature and 50-100 atm unless otherwise noted. Yields were determined spectroscopically unless noted.

Entry	Ketone	% Yield	% es	Ref.
1	 $\text{R} = \text{Me, Et, } i\text{-Pr, } t\text{-Bu}$	≥ 97	≥ 99	[69-71]
2	 $\text{X} = \text{NMe}_2$ $\text{X} = \text{SEt}$	100 42 ^a	98 96	[70]
3	 $\text{R} = \text{Me, } n\text{-Bu, } i\text{-Pr}$	99	≥ 99	[69]
4		99	92	[69]
5	 $\text{R} = \text{TIPS, } n = 1$ $\text{R} = \text{BnO, } n = 2$	100 94	97 99	[70]
6	 $\text{R} = \text{H}$ $\text{R} = \text{Me}$	73 96	99 99	[72]
7	 $\text{X} = \text{NMe}_2$ $\text{X} = \text{OH}$ $\text{X} = \text{CH}_2\text{OH}$	72 100 100	98 96 99	[70]
8	 $\text{R} = i\text{-Pr}$ $\text{R} = \text{Ph}$	83 85	97 97	[70]

^a Isolated yield.

^b 50 psi, 80°

These catalytic reductions are relatively slow, requiring high pressures or high temperatures, and chiral β -ketoesters racemize faster than they can be reduced. As it happens, reduction of one enantiomer is considerably faster than reduction of the other. This is a case of double asymmetric induction (see Section 1.5) applied to a

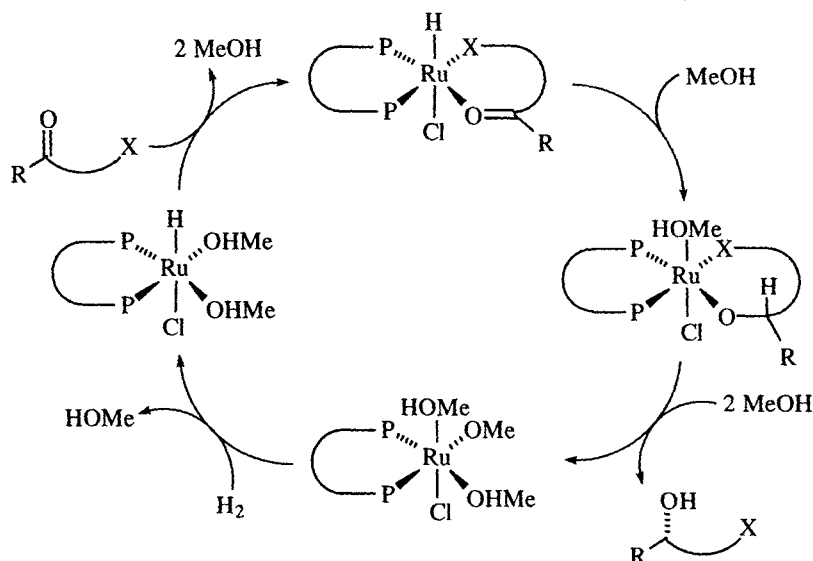


Scheme 7.8. Asymmetric reduction of chiral β -keto esters may be used in an asymmetric transformation of the first kind (dynamic kinetic resolution) [78].

kinetic resolution. Since the enantiomers racemize rapidly, the ruthenium BINAP catalyst can be used to effect an asymmetric transformation of the first kind (see Glossary, section 1.6), as shown in Scheme 7.8a [78]. In this example, the *racemic* β -keto ester is completely converted to the *syn* amino alcohol with a diastereoselectivity (*syn:anti*) of 99:1. The *syn* product is obtained in 94% ee, indicating that of the four possible stereoisomeric products (*syn* and *anti* enantiomers), the major product is 96% of the mixture. The simple explanation for this beautiful result is shown in Scheme 7.8b: racemization under the reaction conditions is fast compared to reduction of either enantiomer, but reduction of the *S*-enantiomer by the *M*-BINAP catalyst (matched pair, addition to the ketone *Si* face) is itself faster than reduction of the *R*-enantiomer (mismatched pair, not shown), so the net result is a draining of the fast racemization equilibrium (Curtin-Hammett principle [79,80]).

The proposed catalytic cycle for these reductions is shown in Scheme 7.9 [76]. In this scheme, it is assumed that the polymeric catalyst precursor $[(\text{BINAP})\text{RuCl}_2]_n$ is dissociated to monomer by the methanolic solvent. Reduction and loss of hydrogen afford the putative catalyst, $(\text{BINAP})\text{RuHCl}(\text{MeOH})_2$. Displacement of the two methanols by the bidentate substrate then sets the stage for the hydrogen transfer step (*vide infra*). Exchange of the alkoxide product with the methanolic solvent and reaction with hydrogen to regenerate the catalyst completes the catalytic cycle. Deuterium labeling experiments showed that the mechanism involves $\text{C}=\text{O}$ reduction, and not the alternative $\text{C}=\text{C}$ reduction of an enol tautomer [78].

The X-ray crystal structures of two ruthenium BINAP complexes have been determined [74,81]. Figure 7.3a illustrates the structural features that are thought to influence stereoselectivity (see also Figure 6.3 and the accompanying discussion). In both crystal structures, the 7-membered chelate ring formed by the *P*-enantiomer of the BINAP ligand and the metal adopt similar conformations and have the pseudo-equatorial phenyl groups occupying the lower left and upper right quadrants, as viewed from the P-Ru-P plane with the BINAP to the rear. The pseudoaxial



Scheme 7.9. Catalytic cycle proposed for the asymmetric reduction of functionalized ketones by ruthenium BINAP catalyst (after ref. [76]).

phenyls are slanted to the rear and would not significantly interact with a ligand bound trans to either phosphorous. For reduction of methyl acetoacetate, *ul* relative topicity is observed (*P*-BINAP catalyst preferentially attacking the *Re* face of the ketone). Assuming that the catalyst is a mononuclear monohydride complex having the hydrogen and chlorine trans, with the substrate chelated to the ruthenium (each carbonyl oxygen being trans to a phosphorous), the chirality sense may be rationalized by the two transition structures illustrated in Figure 7.3b and c. A four-membered transition structure having *lk* topicity (Figure 7.3b) would force the C-4 methyl into the crowded lower left quadrant, while the transition structure with *ul* topicity (Figure 7.3c) is less hindered [76].

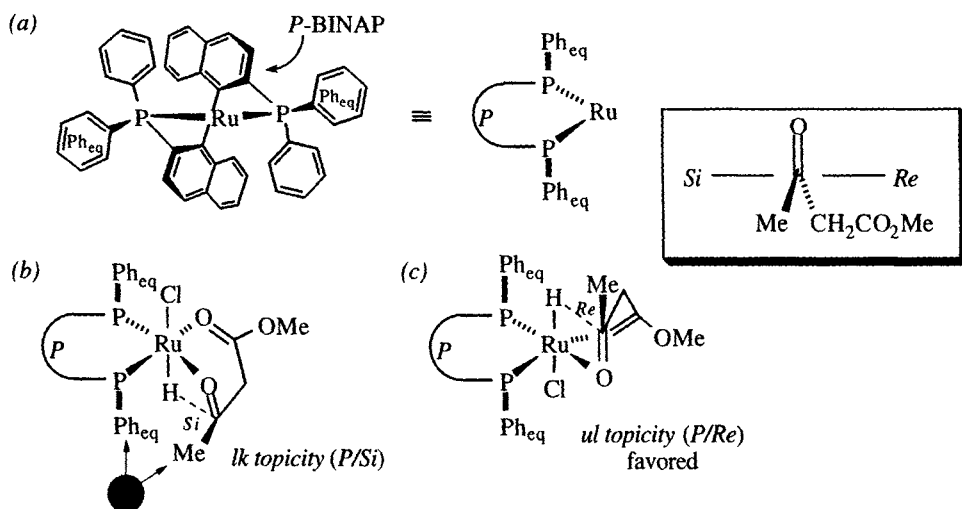


Figure 7.3. (a) Conformation of *P*-BINAP in two crystal structures [74,81]. (b) *lk* Topicity transition structure for asymmetric reduction of methyl acetoacetate. (c) *ul* Topicity transition structure. (After ref. [76]). *Inset*: definition of *Re* and *Si* faces of ketone.

Figure 7.4 illustrates three natural products that have been synthesized using ruthenium(II)-BINAP-mediated ketone reduction as the key step. For pyrenophorin [82] and gloesporone [83], the secondary carbinol is retained, but for indolizidine 223AB, the Mitsunobu reaction is employed to convert the alcohol to an amine [73].

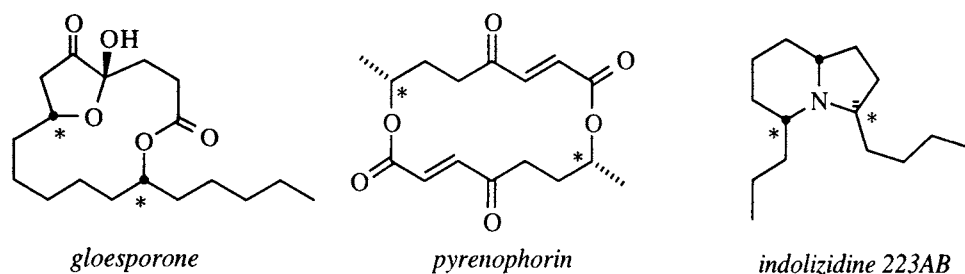
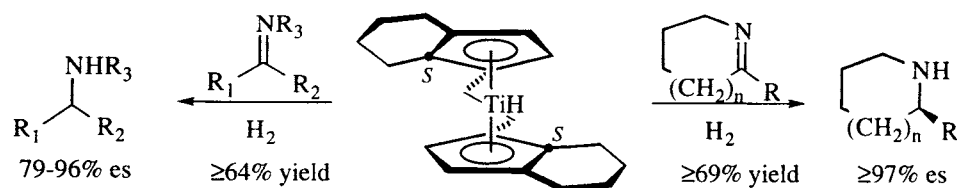


Figure 7.4. Ruthenium(II)-BINAP catalysts have been used as a key step in the asymmetric synthesis of gloesporone [83], pyrenophorin [82], and indolizidine 223AB [73]. Stereocenters formed by asymmetric reduction are indicated (*).

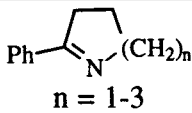
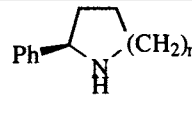
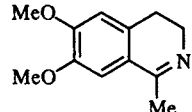
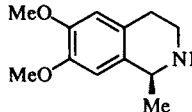
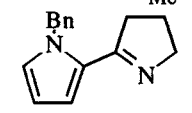
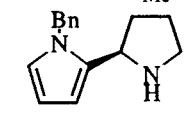
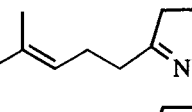
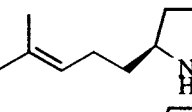
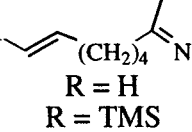
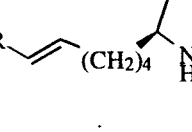
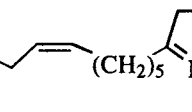
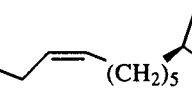
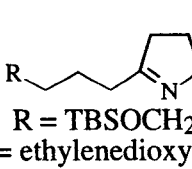
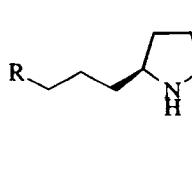
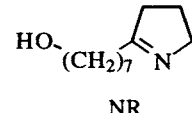
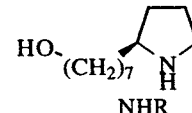
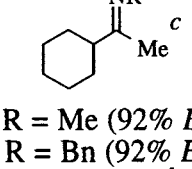
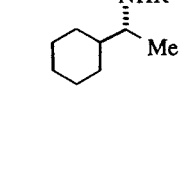
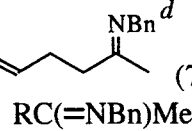
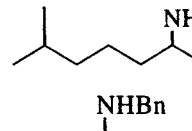
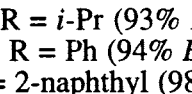
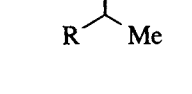
Imine reductions. The asymmetric reduction of carbon–nitrogen double bonds is not possible using ruthenium(II) catalysts, but Buchwald has recently shown that a titanocene catalyst (Scheme 7.10) exhibits good to excellent enantioselectivity in the reduction of imines [84–86] (review: ref. [87]). The reaction can be highly stereoselective for both acyclic and cyclic imines, but since acyclic imines are usually a mixture of *E* and *Z* isomers, and since the imine isomerization is catalyzed by the titanocene, the reaction is not always preparatively useful for acyclic substrates. Examples are listed in Table 7.5. For the cyclic imines (entries 1–8), the enantioselectivities indicated were obtained under hydrogen pressure of 80 psi, at temperatures of 45–65°; higher pressures (500–2000 psi) gave slightly higher enantioselectivities, although reduction of side-chain double bonds occurs.



Scheme 7.10. Titanocene catalyzed asymmetric reduction of imines [85]. In the accompanying discussion, the catalyst shown is designated the *S,S* enantiomer, in accord with the *CIP* rules for describing metal arenes [88]. This is a different designation than that used by Buchwald, however.⁸

⁸ In the original paper describing the preparation of the titanocene catalyst precursor [89], Brintzinger specified the chirality sense of the ansa metallocene by referring to the absolute configuration at C-1 of the indene (the carbon bearing the ethylene bridge), and Buchwald has adopted this usage. However, the *CIP* system states that the chirality sense of the complex should be assigned with reference to the arene ring atom (or in general, the π -complexed atom of any ligand) having the highest CIP rank [88]. In this case, the highest-ranking atom is the C7a (indicated by •), which has the opposite *CIP* designation of C-1. For rules on assigning a *CIP* descriptor to π -complexes, see ref. [90–93]. For another method (Ω +/ Ω -), see ref. [94].

Table 7.5. Examples of asymmetric imine reduction using Buchwald's chiral titanocene catalyst. Reactions were run at 45° and 80 psi, with 5 mol% *S,S* catalyst, unless noted otherwise.

Entry	Imine	Amine	% Yield	% es	Ref.
1	 n = 1-3		71-83	≥99	[84,85, 95]
2			79	97	[84,85, 95]
3			72	>99	[85,95]
4			79	>99	[85,95]
5	 R = H R = TMS		72 73 ^a	>99 >99	[85,95]
6			69 ^b	>99	[85]
7	 R = TBSOCH ₂ R = ethylenedioxy-CH		82 82	>99 >99	[85,95]
8			84	>99	[85,95]
9	 R = Me (92% <i>E</i>) R = Bn (92% <i>E</i>)		85 85	96 71	[84,85]
10	 RC(=NBn)Me ^d		64	81	[85]
11	 R = <i>i</i> -Pr (93% <i>E</i>) R = Ph (94% <i>E</i>) R = 2-naphthyl (98% <i>E</i>)		66 81 82	88 88 85	[84,85]

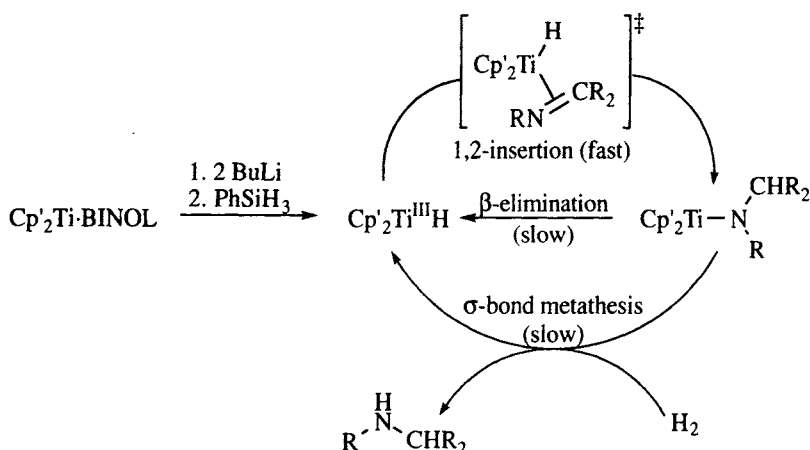
^a Yield includes 5-8% of product having a saturated side chain.

^b Yield includes 13-18% of product having a saturated side chain and 14-18% *E*-olefin.

^c 500 psi H₂

^d 2000 psi H₂.

Examination of the enantioselectivities in Table 7.5 indicates a striking difference in selectivity achieved in the reduction of cyclic (entries 1-8) vs. acyclic imines (entries 9-11). The former is very nearly 100% stereoselective. The simple reason for this is that the acyclic imines are mixtures of *E* and *Z* stereoisomers, which reduce to enantiomeric amines (*vide infra*). The mechanism proposed for this reduction is shown in Scheme 7.11 [86]. The putative titanium(III) hydride catalyst is formed in situ by sequential treatment of the titanocene BINOL complex with butyllithium and phenylsilane. The latter reagent serves to stabilize the catalyst. Kinetic studies show that the reduction of cyclic imines is first order in hydrogen and first order in titanium but zero order in imine. This (and other evidence) is consistent with a fast 1,2-insertion followed by a slow hydrogenolysis (σ -bond metathesis), as indicated [86]. Although β -hydride elimination of the titanium amide intermediate is possible, it appears to be slow relative to the hydrogenolysis.



Scheme 7.11. Proposed catalytic cycle for the titanocene catalyzed reduction of imines [86].

Note the η^2 bonding of the imine to the titanium at the transition state for insertion. The geometry of this complex is critical to the stereoselectivity of the reaction, since it is in this step that the stereocenter in the product is created. A dichlorotitanocene is tetrahedral around titanium, as indicated by the X-ray crystal structure shown in Figure 7.5 [89]. Note the C_2 symmetry of the complex, the orientation of the two cyclohexane moieties in the upper left and lower right quadrants (Figure 7.5b), and the placement of the two chlorines with respect to the cyclohexanes, especially as viewed from the “top” (Figure 7.5d). Based on valence orbital calculations of olefin complexes that are isolobal to the titanium-imine transition structure shown in Scheme 7.11, Buchwald has proposed that the configuration of the titanium in the transition state is similar to that of the dichlorotitanium complex, with one chloride being replaced by a hydride, the other by the η^2 imine ligand, as shown in Figure 7.6 [86]. In a tetrahedral geometry, the imine can only coordinate to the titanium as shown, with the *N*-methylene oriented to the lower left quadrant of the drawing in Figure 7.6a. That this can be the only possible orientation is shown clearly by the top view in Figure 7.6b. This view also

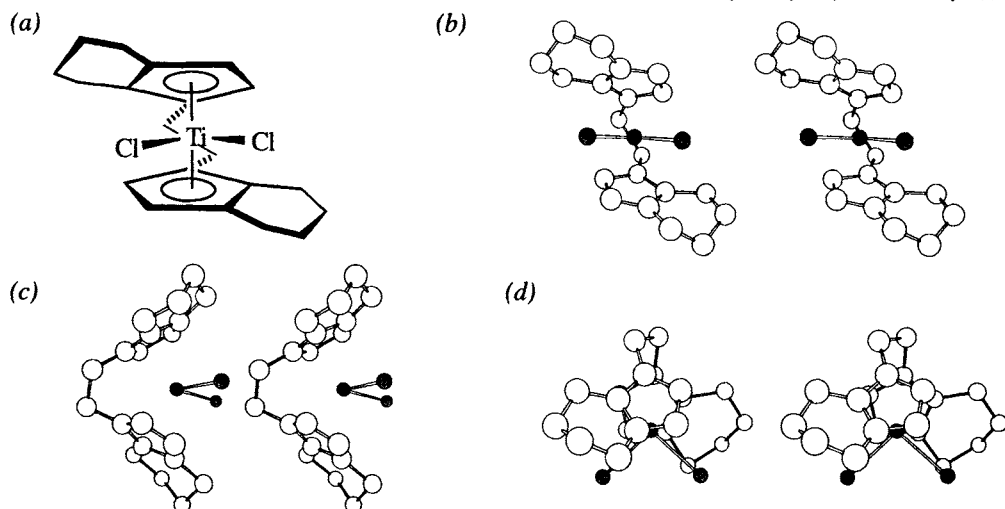


Figure 7.5. Crystal structure of *S,S* ethylene-bis(tetrahydroindenyl)titanium chloride [89]: (a) Perspective drawing of complex. (b) Front stereoview. (c) Side stereoview. (d) Top stereoview.

illustrates positioning of the phenyl in the vacant upper right quadrant, with a minor interaction taking place between C-3 of the heterocycle and the cyclohexyl in the lower right quadrant. This aspect of binding in the transition structure is important in the analysis of the reduction of acyclic imines, as shown in Figure 7.6c and d.

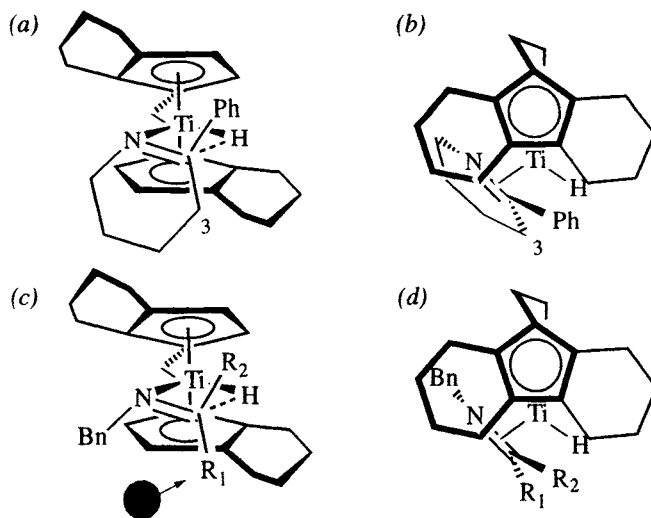
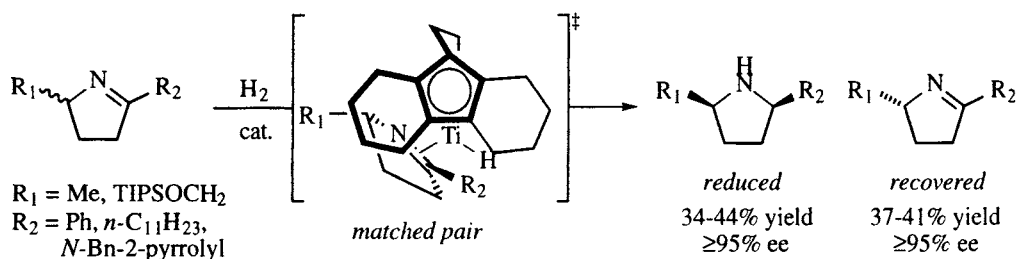


Figure 7.6. Transition structures for titanocene hydride imine reduction [86]: (a) Front view of heterocycle reduction. (b) Top view of heterocycle reduction. (c) Front view of acyclic imine reduction. (d) Top view of imine reduction.

For acyclic imines, note that interchange of R_1 and R_2 in the transition structure is equivalent to an *E/Z* isomerization of the educt. Reduction of cyclohexyl methyl *N*-benzyl imine, using a stoichiometric amount of catalyst affords a 92:8 *R/S* enantiomer ratio that is identical to the 92:8 *E/Z* ratio of the educt (*i.e.*, the reaction

is stereospecific). This is interpreted as follows: the major imine isomer is *E* (R_2 = cyclohexyl, R_1 = methyl). Addition to the *Si* face gives the *R* enantiomer of the amine. With the *Z* imine, R_2 is methyl and R_1 is cyclohexyl. Addition to the *Re* face gives the *S* amine. Entry 9 of Table 7.5 (R = Bn) is the same reaction, but using only 5 mol% of catalyst. Under catalytic conditions, the reaction is no longer stereospecific for two reasons: first, the *E* and *Z* isomers interconvert slowly under the reaction conditions (probably catalyzed by the titanium), and second, the *Z* isomer is reduced faster than the *E* isomer. If the hydrogen pressure is reduced from 2000 psi to 500 psi, the enantioselectivity drops to 71%, consistent with a slower rate of reduction relative to *E/Z* isomerization [86].⁹

The titanocene catalyzed asymmetric imine reduction may be used in kinetic resolutions of racemic pyrrolines [96]. The most efficient kinetic resolution was observed for 5-substituted pyrrolines, and the mechanistic postulate outlined above readily accommodates the experimental results, as shown by the matched pair transition structure in Scheme 7.12 [96].¹⁰ Pyrrolines substituted at the 3- and 4-positions were reduced with excellent enantioselectivity, but kinetic resolution of the starting material was only modest [96].



Scheme 7.12. Kinetic resolution of 5-substituted 1-pyrrolines by asymmetric reduction using the *S,S* chiral titanocene catalyst [96].

7.2 Reduction of carbon-carbon bonds

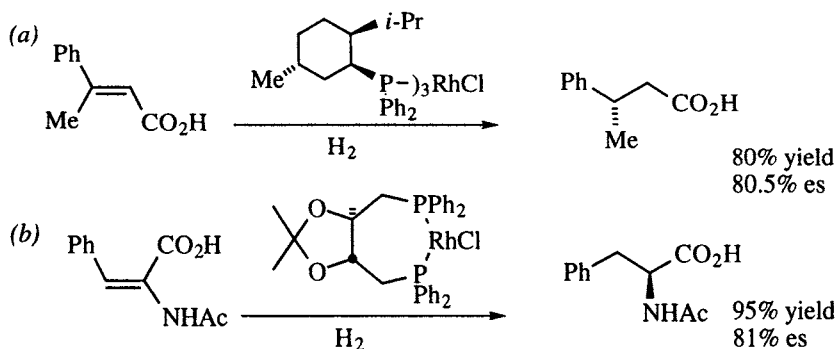
Reduction of a carbon-carbon double bond will produce a chiral product if the olefin is (unsymmetrically) geminally disubstituted. Although hundreds of catalysts having chiral ligands have been synthesized and screened with a number of alkene structural types (reviews: ref. [65,97-107]), the present discussion will focus on only one: the reduction of acetamido cinnamates using soluble rhodium catalysts (reviews: ref. [97,100,108-110]). The development of chiral bisphosphine ligands and the herculean effort that led to the elucidation of the mechanism of this reaction make it an important example for study, since we now know that the major enantiomer of the product arises from a minor (often invisible) component of a pre-equilibrium [109,111]. This aspect of chemical reactivity is an important lesson whose importance cannot be overemphasized: when we strive to understand the

⁹ In contrast, the enantioselectivity of cyclic imine reduction is independent of hydrogen pressure.

¹⁰ In reference [96] the *R,R* enantiomer of the catalyst (*cf* Scheme 7.10) was employed. To maintain consistency with Scheme 7.10 and Figure 7.6, we illustrate the *S,S* catalyst.

forces that govern reactivities and selectivities, we must never overlook the fact that an observable intermediate in a chemical process may not be the one responsible for the observed products.

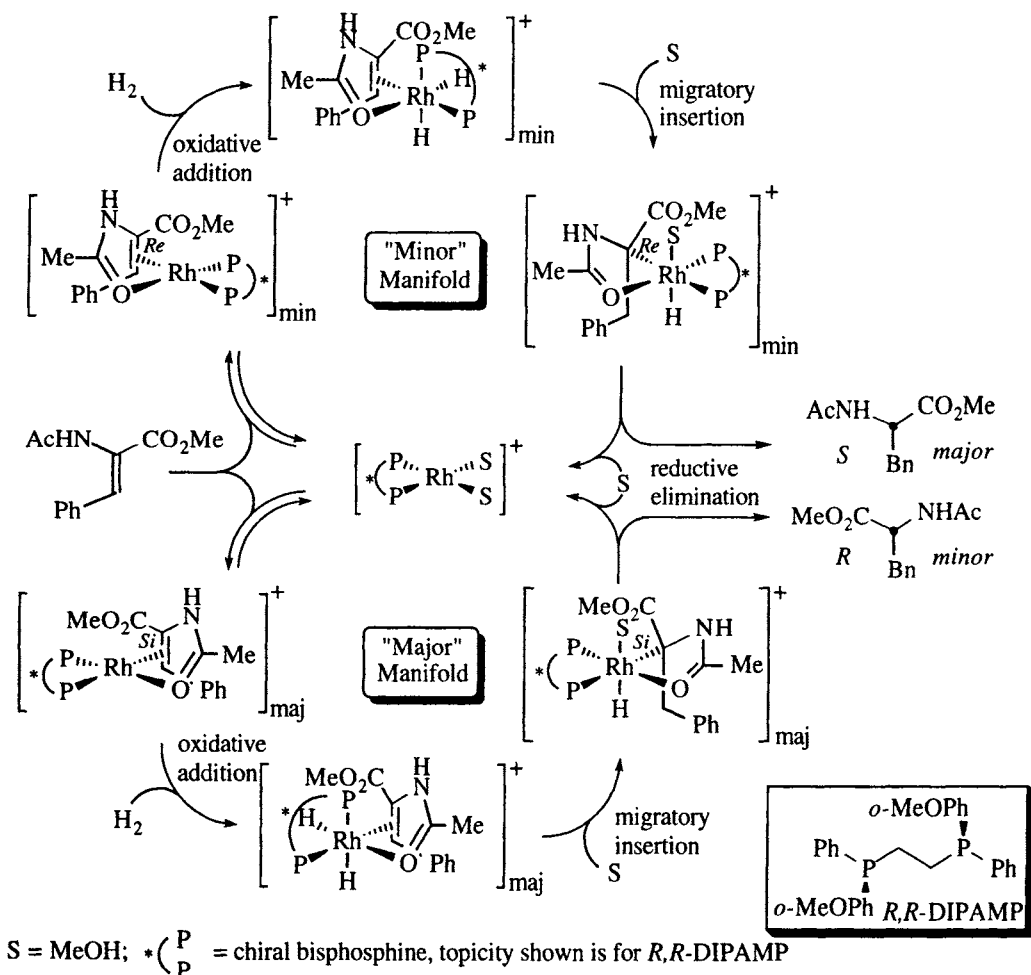
Following Wilkinson's detailed studies of tris-triphenylphosphine rhodium chloride as a soluble catalyst for hydrogenations [112], it did not take long for chemists to realize that chiral phosphines could be substituted for triphenylphosphine so as to effect an asymmetric reduction [113]. Following Mislow's development of a synthesis of chiral phosphine oxides [114], the groups of Knowles [115] and Horner [113] tested methyl phenyl *n*-propyl phosphine in the Wilkinson catalyst system, but found only low selectivities in the reduction of substrates such as α -phenylacrylic acid. These efforts were predicated on the (very reasonable) assumption that the chiral rhodium complex should contain chirality centers at phosphorous (since they are close to the metal). However, this assumption was proven wrong in 1971 when Morrison [116] and Kagan [117] independently showed that ligands such as R^*-PPh_2 (Morrison) and $Ph_2P-R^*-PPh_2$ (Kagan) (where R^* contains a chirality center) were capable of reducing substituted cinnamic acids with enantioselectivities in the 80% (es) range, as shown by the "record-setting" examples in Scheme 7.13. The Kagan ligand, derived from tartaric acid, later became known as "DIOP", and served as the prototype for many more chiral, chelating diphosphine ligands. The Kagan example also demonstrates the utility of an asymmetric reduction protocol for the synthesis of α -amino acids. A similar reaction is now used industrially for the enantioselective production of dihydroxyphenylalanine (DOPA, a drug for treating Parkinson's disease) and aspartame (an artificial sweetener). It can be fairly stated that these spectacular early successes served to heighten optimism for the prospects of asymmetric synthesis in general, and asymmetric catalysis in particular, hopes that have been well rewarded in the interim.



Scheme 7.13. (a) Morrison's asymmetric reduction of β -methyl cinnamic acid [116]. (b) Kagan's asymmetric reduction of *N*-acetyl dehydrophenylalanine and the debut of the DIOP ligand [117].

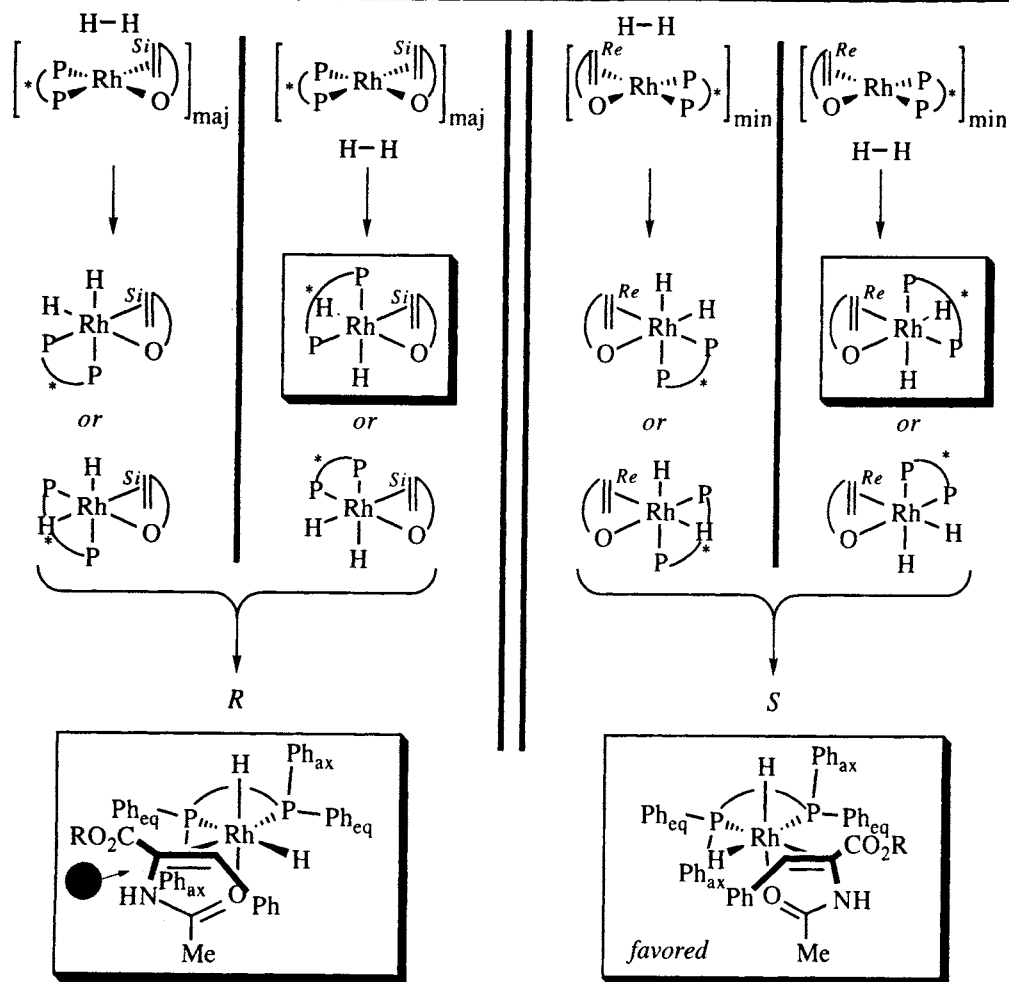
These examples were followed with a continuous stream of ligands (that continues to this day: cf. ref. [66,105,107,108,118-120]) that were tested with rhodium and other metals in asymmetric reductions and other reactions catalyzed by transition metals [102-104,121]. Simultaneously, studies of the mechanism of the asymmetric hydrogenation were pursued, most aggressively in the labs of Halpern

and Brown. The currently accepted mechanism is shown in Scheme 7.14 [111]. The substrate (methyl *Z*-acetamidocinnamate, middle left) displaces two solvent molecules from the cationic rhodium catalyst (center) in an equilibrium that favors the diastereomer in which the rhodium is bound to the *Si* face (at C-2) of the alkene [122]. This equilibrium defines the "major" and "minor" manifolds of the reaction. The sequence of oxidative addition of dihydrogen, migratory insertion, and reductive elimination, completes the cycle in both manifolds. With some bisphosphines, both of the initially formed diastereomeric complexes are visible by NMR; with others, signals from the minor diastereomer are lost in the noise. Each subsequent reaction is irreversible, but at low temperature the rhodium alkyl hydride product of migratory insertion can be intercepted and characterized spectroscopically [123,124]. Surprisingly, the intercepted complex (leading to the *S* product) has the metal on the *Re* face of C-2! Thus, the major product of the reduction is produced by oxidative addition of dihydrogen to the minor diastereomer of the catalyst-substrate complex [111,123].



Scheme 7.14. Mechanism of asymmetric hydrogenation of *N*-acetyl dehydrophenylalanine [111].

At temperatures above -40° , the rate-determining step of the reaction is the oxidative addition of hydrogen to the catalyst-substrate complex. Because the interconversion of the two diastereomeric catalyst-substrate complexes is fast relative to the rate of oxidative addition [111], and because the migratory insertion and reductive elimination steps are kinetically invisible, the complex equilibria in Scheme 7.14 reduce to a classic case of Curtin-Hammett kinetics [80], whereby the



Scheme 7.15. Possible orientations for oxidative addition of dihydrogen to the major (left) and minor (right) diastereomers of the catalyst-substrate complex (for simplicity, the linkages connecting the atoms bonded to the metal are indicated with a curved line). The boxed structures are the only octahedral structures that are not encumbered by severe non-bonded interactions; they are redrawn at the bottom with the bisphosphine to the rear and in the horizontal plane. The topicity illustrated is for ligands having the structure of Figure 7.8, such as *R,R* DIPAMP, *R,R*-DIOP, or *R,R* CHIRAPHOS (see Figure 7.8).

'faces' are exposed to a ligand coordinated at a site towards the viewer, while the two axial phenyls expose 'edges'. This conformation produces two crowded quadrants (those having the axial phenyls) and two vacant quadrants, as shown in Figure 7.8. Structural features similar to this have turned up in the interim in the structures of numerous other ligands, and can be conveniently used to explain the stereoselectivity of a number of metal-catalyzed reactions (*cf.* Figures 4.18, 6.3, 6.10, 6.20, 6.21, 7.3, 7.6).¹¹

For the asymmetric hydrogenation, both substrate-catalyst complexes are square-planar, and hydrogen could, in principle, add from either the top or the bottom of

¹¹ For a recent leading reference to these structural features, see ref. [126,127]

either complex, as illustrated in Scheme 7.15. From a molecular orbital standpoint, there is no reason to expect any one of these four possibilities to dominate. Indeed, it is likely that the oxidative addition of dihydrogen occurs stepwise, and that the hydrogen binds “edgewise” initially (making a square pyramid complex), followed by H–H cleavage to form the octahedral dihydride product. Further, it is likely that the dihydrogen associates with the metal many times before H–H bond cleavage occurs.¹² Lacking an electronic rationale, the only other possible explanation is that the movement of the ligands (as the oxidative addition proceeds) is determinant.

Scheme 7.15 illustrates the eight possible octahedral complexes that could arise by addition of dihydrogen to either the top or the bottom of the two square complexes. Each is drawn so that the orientation of the substrate remains unchanged, and one of the phosphines is moved trans to the incoming hydrogen. A molecular mechanics investigation [129] indicates that only two of the eight structures are viable (boxed, redrawn at the bottom of Scheme 7.15); all the others suffer severe nonbonded interactions between ligands. Note the similarity of the two boxed structures: in both, a hydride is trans to the chelating oxygen and cis to both phosphorous atoms. The double bond and the second hydride are then meridonal with respect to the two phosphorous atoms. The reason for the difference in stability can be seen by examining the orientation of the substrate relative to the axial phenyls: in the favored configuration, the substrate occupies the less crowded “lower right” quadrant. It is implicit in this analysis that the energetic consequences of these various structural features must be felt in the competing transition states for oxidative addition.

Two factors contribute to the success of this reaction: the outstanding enantioselectivity achieved, and efficiency of the catalyst (*i.e.*, high turnover). The above analysis emphasizes only the former, but the latter also varies with the nature of the chiral bisphosphine ligand and the structure of the substrate. The structural features of the substrate and the catalyst are mutually optimal in the example cited above. Perturbation of any of these features usually lowers either the enantioselectivity or the turnover rate. The range of substrates that are amenable to asymmetric hydrogenation with this catalyst system is, therefore, limited. Figure 7.9 illustrates the classes of substrate that can be accommodated by cationic rhodium bisphosphine catalysts [104]. For a more extensive summary, see ref. [110].

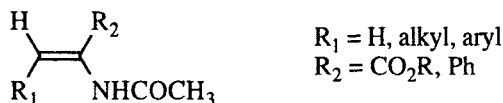


Figure 7.9. Substrate tolerance in the asymmetric hydrogenation (after ref. [104]).

¹² Hoff has shown that the rate of dissociation of a tungsten-dihydrogen complex is at least one order of magnitude faster than the rate of oxidative addition (H–H bond cleavage) to a dihydride complex [128].

7.3 Hydroborations

The first asymmetric synthesis to achieve >90% optical yield was Brown's hydroboration of *cis* alkenes with diisopinocampheylborane (Ipc_2BH , Figure 7.10) in 1961 [130,131]. The reagent was prepared by hydroboration of α -pinene of ~90% ee; 2-butanol obtained from hydroboration/oxidation of *cis*-2-butene had an optical purity of 87%, indicating an optical yield of 90%. *cis*-3-Hexene was hydroborated in ~100% optical yield. Since then, simple methods for the enantiomer enrichment of Ipc_2BH (and IpcBH_2) have been developed [132-134], and enantioselectivities have been evaluated more carefully with the purified material. For example, Ipc_2BH of 99% ee¹³ affords 2-butanol (from *cis*-2-butene) in 98% ee and 3-hexanol (from *cis*-3-hexene) in 93% ee, both determined by rotation (see Table 7.6, entries 1 and 5) [132].¹⁴

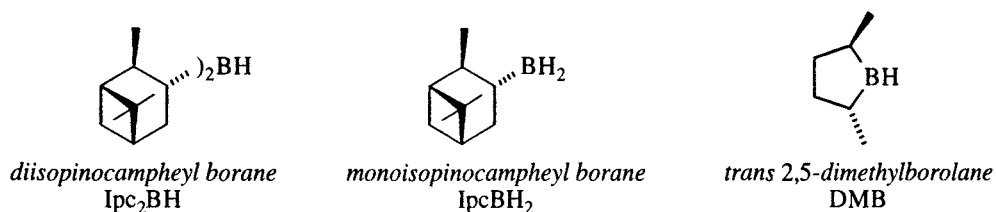


Figure 7.10. Chiral hydroborating reagents: Ipc_2BH [130-134], IpcBH_2 [133,135]; DMB [136].

Today, Ipc_2BH is still as good a reagent as any for achieving enantioselective hydroboration of *cis* alkenes (Table 7.6, entries 1, 2, 6, 7, 10, 12-17; reviews: [2,137-139]). However, it does not afford good enantioselectivities with *trans*-disubstituted or trisubstituted alkenes. For these classes of compounds, monoisopinocampheylborane, IpcBH_2 (Figure 7.10), gives good selectivities, as indicated by the examples in Table 7.6, entries 4, 8, and 11 [135]; recrystallization of the intermediate borane may be used to purify the major borane diastereomer in some cases (Table 7.6, entries 2, 18, 20, 22, 24, and 26), and serves to improve the overall enantioselectivity of the process [133].

In 1985 [136], Masamune introduced *trans*-2,5-dimethylborolane (Figure 7.10) as a chiral hydroborating agent that works well for *cis* and *trans* disubstituted and trisubstituted alkenes (Table 7.6, entries 3, 5, 7, 9, 19, 21, and 23). Although this reagent is the most versatile yet invented, its preparation is sufficiently cumbersome that its synthetic utility is not great. On the other hand, the conformational rigidity of this reagent allows us to postulate a reasonable transition structure to account for the topicity of the hydroboration (Scheme 7.16). Specifically, when $\text{R}_1 \neq \text{H}$, and either R_2 or $\text{R}_3 = \text{H}$, the boron of the *R,R*-borolane adds preferentially to the *Si* face of the alkene carbon. Good stereoselectivity will result when either R_2 or R_3 (or both) are $\neq \text{H}$, since the carbon which is attacked by boron determines the stereoselectivity. Conversely, if $\text{R}_1 = \text{H}$, there is little difference in energy between

¹³ This is the enantiomeric purity of isopinocampheol produced by oxidation of the purified Ipc_2BH , measured by rotation [132].

¹⁴ The discrepancy between the optical yields using enantiopure α -pinene and that of ~90% ee is probably due experimental error in the measurement of rotations.

Table 7.6. Examples of enantioselective hydroborations. The "Reagent" column refers to the structures in Figure 7.10. The "% es" column reflects the overall enantioselectivity of the process, including any diastereomeric enrichment, and is corrected for the enantiomeric purity of the borane.

Entry	Alkene	Reagent	% Yield	% es	Ref.
1	<i>cis</i> -2-butene	Ipc ₂ BH	74	99	[130-132]
2	"	IpcBH ₂	78	99	[133]
3	"	DMB	75	97	[136]
4	<i>trans</i> -2-butene	IpcBH ₂	73	86	[135]
5	"	DMB	71	100	[136]
6	<i>cis</i> -3-hexene	Ipc ₂ BH	68-81	95-96	[130-132]
7	"	DMB	83	100	[136]
8	<i>trans</i> -3-hexene	IpcBH ₂	83	87	[135]
9	"	DMB	83	>99	[136]

the illustrated transition structure and an alternative one in which R_2 and R_3 are interchanged. In fact, for 1,1-disubstituted alkenes, none of the reagents of Figure 7.10 affords products in greater than 10% ee ($\leq 55\%$ es).

The conformational mobility around the B–C bond(s) in IpcBH_2 and Ipc_2BH complicate the analysis for these terpene-derived boranes, but Figure 7.11 gives a simplified picture. Using *ab initio* techniques, Houk and coworkers [141] located the transition structures for the hydroboration of simple alkenes, and found that the most consistent feature of the most stable transition structures has the auxiliary (R^*) and the substituent on carbon (R) anti to each other, as shown in Figure 7.11a. Analysis of the conformational motion of the B– R^* bond revealed that the substituents on boron prefer to be staggered with respect to the forming C–B bond. Furthermore, the most stable position is anti to this bond. The so-called “outside” position is less encumbered sterically than the “inside” position, and the difference in energy between these two is affected by whether the alkene is *cis* or *trans* (Figure 7.11b). In Figure 7.11c the pinene substituent is reduced to a shorthand notation of Small (H), Medium, and Large substituents on the carbon bearing the boron.

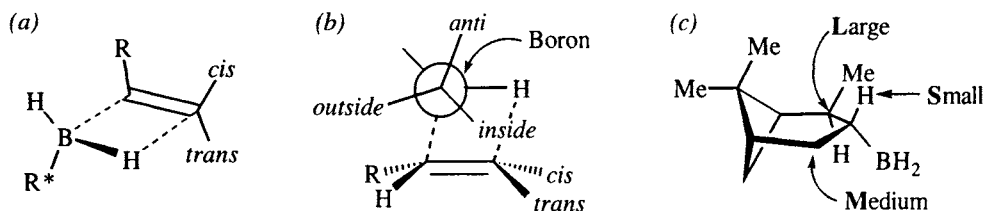


Figure 7.11. Terminology definitions for hydroboration transition structures [141]: (a) The auxiliary may be either syn or anti to the alkene substituents, but anti to the substituent (R) on the nearest carbon. (b) A stereocenter attached to boron, in a staggered conformation with respect to the forming C–B bond, has substituents in *anti*, *inside*, and *outside* positions. (c) Definition of the Large, Medium, and Small substituents of IpcBH_2 .

With these generalizations in mind, it is possible to qualitatively¹⁵ rationalize the results with IpcBH_2 and Ipc_2BH . The more easily understood example, of course, is IpcBH_2 , since there is only one pinene moiety involved. This reagent is most selective with *trans* alkenes, so this olefin-type is illustrated first. The lowest energy (molecular mechanics) transition structure for addition of boron to the *Si* face of the alkene (Figure 7.12a) has the pinene anti to R (methyl), and has the small, medium, and large ligands in the most stable positions relative to the newly forming C–B bond: *L-anti*, *M-outside*, and *Small(H)-inside*. In contrast, the transition structure for addition to the *Re* face (Figure 7.12b) has *L* in the less favorable *outside* position [141]. Note that in both of these structures the *inside* position is in close proximity to the second methyl (R) group, which increases the destabilization of any conformer in which either *M* or *L* occupy the *inside* position. IpcBH_2 is also fairly selective with trisubstituted alkenes (Table 7.6), and the transition structures of Figure 7.12 show why this should be the case: an additional substituent in the *cis*

¹⁵ Houk, et al, note that the magnitude of the experimentally observed selectivities do not correspond to the energy differences their molecular mechanics calculations indicate, so this analysis and the calculated transition structures may only be taken as a first approximation [141].

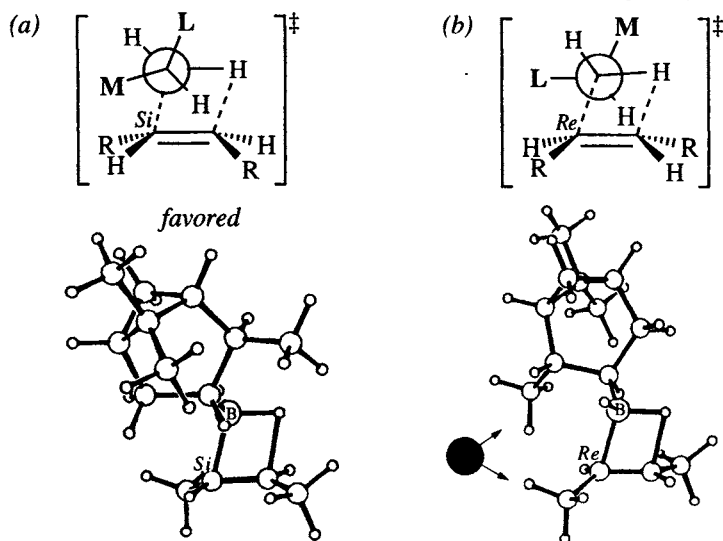


Figure 7.12. Transition structures for the asymmetric hydroboration of *trans*-2-butene with IpcBH_2 . Reprinted with permission from ref. [141], copyright 1984 Elsevier Science, Ltd.

position (*cf.* Figure 7.11a,b) imposes no additional crowding on the transition structure. On the other hand, IpcBH_2 is much less selective with *cis* alkenes. Here, the position of the alkyl group is moved away from its close proximity to the *inside* position, and a number of other transition structures become feasible [141].

For hydroborations with Ipc_2BH , there are two pinene moieties to consider. Ipc_2BH is only selective for *cis* alkenes, and the alkene substituents (R in Figure 7.13a) must be near one of them (R^* in Figure 7.13a). Houk, et al., find that there is only one conformation that the two pinenes may adopt relative to each other, and that is shown schematically in Figure 7.13b [141]. In the conformation shown, the olefin can align itself with the B-H bond and have the two R groups oriented either toward the proximal or distal pinene. Note that the proximal pinene has the Small hydrogen in the *inside* position, whereas the Large substituent of the distal pinene is

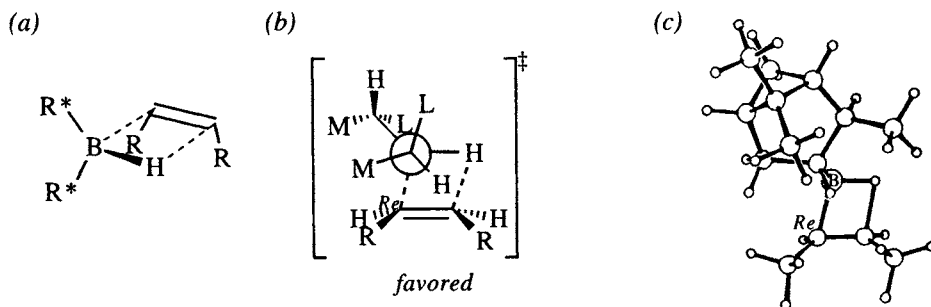


Figure 7.13. Transition structure for hydroboration of a *cis* alkene with Ipc_2BH . (a) The alkene substituents must be syn to one of the pinenes (R^*). (b) Schematic representation of the lowest energy conformation. (c) Molecular mechanics - derived structure, with the rear (distal) pinene deleted for clarity. Reprinted with permission from ref. [141], copyright 1984, Elsevier Science, Ltd.

in the crowded *inside* position. The alkene is least hindered in the orientation shown in Figure 7.13b. Figure 7.13c shows the transition structure with the distal pinene deleted for clarity [141]. Note that in this structure, the alkene substituent is oriented toward the proximal pinene (with respect to the 4-membered ring), and it is therefore clear why Ipc_2BH preferentially attacks the *Re* face (Figure 7.13). This is in contrast to IpcBH_2 , which prefers the *Si* face (Figure 7.12), because the alkene substituent is anti to the pinene.

7.4 References

1. H. C. Brown; P. K. Jadhav; A. K. Mandal *Tetrahedron* **1981**, 37, 3574-3587.
2. H. C. Brown; B. Singaram *Pure Appl. Chem.* **1987**, 59, 879-894.
3. R. C. Larock *Comprehensive Organic Transformations. A Guide to Functional Group Preparations*; VCH: New York, 1989.
4. H. C. Brown; W. S. Park; B. T. Cho; P. V. Ramachandran *J. Org. Chem.* **1987**, 52, 5406-5412.
5. A. A. Bothner-by *J. Am. Chem. Soc.* **1951**, 73, 846.
6. J. D. Morrison; H. S. Mosher In *Asymmetric Organic Reactions*; Prentice-Hall: Englewood Cliffs, NJ, 1971, p 202-215.
7. E. R. Grandbois; S. I. Howard; J. D. Morrison In *Asymmetric Synthesis*; J. D. Morrison, Ed.; Academic: Orlando, 1983; Vol. 2, p 71-79.
8. M. Nishizawa; R. Noyori In *Comprehensive Organic Synthesis. Selectivity, Strategy, and Efficiency in Modern Organic Chemistry*; B. M. Trost, I. Fleming, Eds.; Pergamon: Oxford, 1991; Vol. 8, p 159-182.
9. J. Seyden-Penne *Reductions by the Alumino- and Borohydrides in Organic Synthesis*; VCH: New York, 1991.
10. R. Noyori; R. Tomino; I. Tomino; Y. Tanimoto *J. Am. Chem. Soc.* **1979**, 101, 3129-3131.
11. M. Nishizawa; M. Yamada; R. Noyori *Tetrahedron Lett.* **1981**, 22, 247-250.
12. R. Noyori; I. Tomino; Y. Tanimoto; M. Nishizawa *J. Am. Chem. Soc.* **1984**, 106, 6709-6716.
13. R. Noyori; I. Tomino; M. Yamada; M. Nishizawa *J. Am. Chem. Soc.* **1984**, 106, 6717-6725.
14. D. Seebach; A. K. Beck; R. Dahinden; M. Hoffmann; F. N. M. Kühnle *Croatia Chem. Acta* **1996**, in press.
15. A. K. Beck; R. Dahinden; F. N. M. Kühnle In *ACS Symposium Series. Reduction in Organic Chemistry*; A. F. Abdel-Magid, Ed.; American Chemical Society: Washington, D. C., 1996.
16. J. March In *Advanced Organic Chemistry, 4th ed.*; Wiley-Interscience: New York, 1992, p 145.
17. K. Matsuki; H. Inoue; M. Takeda *Tetrahedron Lett.* **1993**, 34, 1167-1170.
18. J. C. Fiaud; H. B. Kagan *Bull. Soc. Chim. Fr.* **1969**, 2742-2743.
19. S. Wallbaum; J. Martens *Tetrahedron Asymmetry* **1992**, 3, 1475-1504.
20. L. Deloux; M. Srebnik *Chem. Rev.* **1993**, 93, 763-784.
21. A. Hirao; S. Itsuno; S. Nakahama; N. Yamazaki *J. Chem. Soc., Chem. Commun.* **1981**, 315-317.
22. S. Itsuno; A. Hirao; S. Nakahama; N. Yamazaki *J. Chem. Soc., Perkin Trans. 1* **1983**, 1673-1676.
23. S. Itsuno; K. Ito; A. Hirao; S. Nakahama *J. Chem. Soc., Chem. Commun.* **1983**, 469-470.
24. S. Itsuno; M. Nakano; K. Miyazaki; H. Masuda; K. Ito *J. Chem. Soc., Perkin Trans. 1* **1985**, 2039-2044.
25. S. Itsuno; K. Ito; A. Hirao; S. Nakahama *J. Chem. Soc., Perkin Trans. 1* **1984**, 2887-2893.
26. S. Itsuno; K. Ito; A. Hirao; S. Nakahama *J. Org. Chem.* **1984**, 49, 555-557.
27. E. J. Corey; R. K. Bakshi; S. Shibata *J. Org. Chem.* **1988**, 53, 2861-2863.

28. S. Itsuno; Y. Sakurai; K. Ito; A. Hirao; S. Nakahama *Bull. Chem. Soc. Jpn.* **1987**, *60*, 395-396.
29. E. J. Corey; R. K. Bakshi; S. Shibata *J. Am. Chem. Soc.* **1987**, *109*, 5551-5553.
30. E. J. Corey; R. K. Bakshi; S. Shibata; C.-P. Chen; V. K. Singh *J. Am. Chem. Soc.* **1987**, *109*, 7925-7926.
31. E. J. Corey; J. O. Link *Tetrahedron Lett.* **1989**, *30*, 6275-6278.
32. E. J. Corey; M. Azomioara; S. Sarshar *Tetrahedron Lett.* **1992**, *33*, 3429-3430.
33. D. J. Mathre; T. K. Jones; L. C. Xavier; T. J. Blacklock; R. A. Reamer; J. J. Mohan; E. T. T. Jones; K. Hoogsteen; M. W. Baum; E. J. J. Grabowski *J. Org. Chem.* **1991**, *56*, 751-762.
34. V. Nevalainen *Tetrahedron Asymmetry* **1991**, *2*, 429-435.
35. D. K. Jones; D. C. Liotta; I. Shinkai; D. J. Mathre *J. Org. Chem.* **1993**, *58*, 799-801.
36. G. J. Quallich; J. F. Blake; T. M. Woodall *J. Am. Chem. Soc.* **1994**, *116*, 8516-8525.
37. V. Nevalainen *Tetrahedron Asymmetry* **1992**, *3*, 921-932.
38. E. J. Corey; J. O. Link *J. Am. Chem. Soc.* **1992**, *114*, 1906-1908.
39. E. J. Corey; J. O. Link; Y. Shao *Tetrahedron Lett.* **1992**, *33*, 3435-3438.
40. E. J. Corey; J. O. Link *Tetrahedron Lett.* **1992**, *33*, 3431-3434.
41. E. J. Corey; C. J. Helal *Tetrahedron Lett.* **1993**, *34*, 5227-5230.
42. E. J. Corey; J. O. Link *Tetrahedron Lett.* **1992**, *33*, 4141-4144.
43. E. J. Corey; R. K. Bakshi *Tetrahedron Lett.* **1990**, *31*, 611-614.
44. P. Beak; S. T. Kerrick; S. Wu; J. Chu *J. Am. Chem. Soc.* **1994**, *116*, 3231-3239.
45. T. K. Jones; J. J. Mohan; L. C. Xavier; T. J. Blacklock; D. J. Mathre; P. Sohar; E. T. T. Jones; R. A. Reamer; F. E. Roberts; E. J. J. Grabowski *J. Org. Chem.* **1991**, *56*, 763-769.
46. M. M. Midland *Chem. Rev.* **1989**, *89*, 1553-1561.
47. H. C. Brown; P. V. Ramachandran *Pure Appl. Chem.* **1991**, *63*, 307-316.

- York, 1993, p 1-39.
66. R. Noyori *Asymmetric Catalysis in Organic Synthesis*; Wiley-Interscience: New York, 1994.
67. H. Brunner; H. Nishiyama; K. Itoh In *Catalytic Asymmetric Synthesis*; I. Ojima, Ed.; VCH: New York, 1993, p 303-322.
68. R. Noyori In *Asymmetric Catalysis in Organic Synthesis*; Wiley-Interscience: New York, 1994, p 124-131.
69. R. Noyori; T. Ohkuma; M. Kitamura; H. Takaya; N. Sayo; H. Kumobayashi; S. Akutagawa *J. Am. Chem. Soc.* **1987**, *109*, 5856-5858.
70. M. Kitamura; T. Ohkuma; S. Inoue; N. Sayo; H. Kumobayashi; S. Akutagawa; T. Ohta; H. Takaya; R. Noyori *J. Am. Chem. Soc.* **1988**, *110*, 629-631.
71. M. Kitamura; M. Tokunaga; T. Ohkuma; R. Noyori *Tetrahedron Lett.* **1991**, *32*, 4163-4166.
72. D. F. Taber; L. J. Silverberg *Tetrahedron Lett.* **1991**, *32*, 4227-4230.
73. D. F. Taber; P. B. Dekker; L. J. Silverberg *J. Org. Chem.* **1992**, *57*, 5990-5994.
74. K. Mashima; K. Kusano; T. Ohta; R. Noyori; H. Takaya *J. Chem. Soc., Chem. Commun.* **1989**, 1208-1210.
75. K. Mashima; K. Kusano; N. Sato; Y. Matsumura; K. Nozaki; H. Kumobayashi; N. Sayo; Y. Hori; T. Ishikazi; S. Akutagawa; H. Takaya *J. Org. Chem.* **1994**, *59*, 3064-3076.
76. R. Noyori In *Asymmetric Catalysis in Organic Synthesis*; Wiley-Interscience: New York, 1994, p 63-66.
77. M. J. Burk; T. G. P. Harper; C. S. Kalberg *J. Am. Chem. Soc.* **1995**, *117*, 4423-4424.
78. R. Noyori; T. Ikeda; T. Ohkuma; M. Widhalm; M. Kitamura; H. Takaya; S. Akutagawa; N. Sayo; T. Saito; T. Taketomi; H. Kumobayashi *J. Am. Chem. Soc.* **1989**, *111*, 9134-9135.
79. D. Y. Curtin *Rec. Chem. Progr.* **1954**, *15*, 111-128.
80. J. I. Seeman *Chem. Rev.* **1983**, *83*, 83-134.
81. T. Ohta; H. Takaya; R. Noyori *Inorg. Chem.* **1988**, *27*, 566-569.
82. J. E. Baldwin; R. M. Adlington; S. H. Ramcharitar *Synlett* **1992**, 875-877.
83. S. L. Schreiber; S. E. Kelly; J. A. Porco, Jr.; T. Sammakia; E. M. Suh *J. Am. Chem. Soc.* **1988**, *110*, 6210-6218.
84. C. A. Willoughby; S. L. Buchwald *J. Am. Chem. Soc.* **1992**, *114*, 7562-7564.
85. C. A. Willoughby; S. L. Buchwald *J. Am. Chem. Soc.* **1994**, *116*, 8952-8965.
86. C. A. Willoughby; S. L. Buchwald *J. Am. Chem. Soc.* **1994**, *116*, 11703-11714.
87. C. Bolm *Angew. Chem. Int. Ed. Engl.* **1993**, *32*, 232-233.
88. R. S. Cahn; C. K. Ingold; V. Prelog *Angew. Chem. Int. Ed. Engl.* **1966**, *5*, 385-415, 511.
89. F. R. W. P. Wild; L. Zsolnai; G. Huttner; H. H. Brintzinger *J. Organomet. Chem.* **1982**, *232*, 233-247.
90. K. Schlögl In *Topics in Stereochemistry*; E. L. Eliel, N. L. Allinger, Eds.; Wiley-Interscience: New York, 1967; Vol. 1, p 39-91.
91. T. E. Sloan In *Topics in Stereochemistry*; G. L. Geoffroy, Ed.; Wiley-Interscience: New York, 1981; Vol. 12, p 1-36.
92. E. L. Eliel; S. H. Wilen; L. N. Mander In *Stereochemistry of Organic Compounds*; Wiley-Interscience: New York, 1994; Vol. Ch. 14, p 1121-2.
93. G. Helmchen In *Stereoselective Synthesis*; G. Helmchen, R. W. Hoffmann, J. Mulzer, E. Schaumann, Eds.; Georg Thieme: Stuttgart, 1995; Vol. E21a, p 1-74.
94. K. Hortmann; H.-H. Brintzinger *New J. Chem.* **1992**, *16*, 51-55.
95. C. A. Willoughby; S. L. Buchwald *J. Org. Chem.* **1993**, *58*, 7627-7629.
96. A. Viso; N. E. Lee; S. L. Buchwald *J. Am. Chem. Soc.* **1994**, *116*, 9373-9374.
97. H. B. Kagan *Pure Appl. Chem.* **1975**, *43*, 401-421.
98. J. D. Morrison; W. F. Masler; M. K. Neuberger *Adv. in Catal.* **1976**, *25*, 81-124.
99. V. Caplar; G. Comisso; V. Sunjic *Synthesis* **1981**, 85-116.
100. W. S. Knowles *Acc. Chem. Res.* **1983**, *16*, 106-112.
101. H. Takaya; R. Noyori In *Comprehensive Organic Synthesis. Selectivity, Strategy, and Efficiency in Modern Organic Chemistry*; B. M. Trost, I. Fleming, Eds.; Pergamon: Oxford,

- 1991; Vol. 8, p 443-469.
102. H. Brunner *Synthesis* **1988**, 645-654.
103. S. L. Blystone *Chem. Rev.* **1989**, 89, 1663-1679.
104. H. B. Kagan *Bull. Soc. Chim. Fr.* **1988**, 846-853.
105. R. Noyori; H. Takaya *Acc. Chem. Res.* **1990**, 23, 345-350.
106. R. Noyori In *Asymmetric Catalysis in Organic Synthesis*; Wiley-Interscience: New York, 1994, p 16-94.
107. K. Inoguchi; S. Sakuraba; K. Achiwa *Synlett* **1992**, 169-178.
108. H. B. Kagan In *Asymmetric Synthesis*; J. D. Morrison, Ed.; Academic: Orlando, 1985; Vol. 5, p 1-39.
109. J. Halpern In *Asymmetric Synthesis*; J. D. Morrison, Ed.; Academic: Orlando, 1985; Vol. 5, p 41-69.
110. K. E. Koenig In *Asymmetric Synthesis*; J. D. Morrison, Ed.; Academic: Orlando, 1985; Vol. 5, p 71-101.
111. C. R. Landis; J. Halpern *J. Am. Chem. Soc.* **1987**, 109, 1746-1754.
112. J. A. Osborn; F. H. Jardine; J. F. Young; G. Wilkinson *J. Chem. Soc. (A)* **1966**, 1711-1732.
113. L. Horner; H. Büthe; H. Siegel *Tetrahedron Lett.* **1968**, 4023-4026.
114. O. Korpium; R. A. Lewis; J. Chickos; K. Mislow *J. Am. Chem. Soc.* **1968**, 90, 4842-4846.
115. W. S. Knowles; M. J. Sabacky *J. Chem. Soc., Chem. Commun.* **1968**, 1445-1446.
116. J. D. Morrison; R. E. Burnett; A. M. Aguiar; C. J. Morrow; C. Phillips *J. Am. Chem. Soc.* **1971**, 93, 1301-1303.
117. T. P. Dang; H. B. Kagan *Chem. Commun.* **1971**, 481.
118. M. J. Burk; J. E. Feaster; R. L. Harlow *Tetrahedron Asymmetry* **1991**, 2, 569-592.
119. *Catalytic Asymmetric Synthesis*; I. Ojima, Ed.; VCH: New York, 1993.
120. M. J. Burk; M. F. Gross; J. P. Martinez *J. Am. Chem. Soc.* **1995**, 117, 9375-9376.
121. R. Noyori *Science* **1990**, 248, 1194-1199.
122. A. S. C. Chan; J. J. Pluth; J. Halpern *J. Am. Chem. Soc.* **1980**, 102, 5952-5954.
123. J. M. Brown; P. A. Chaloner *J. Chem. Soc., Chem. Commun.* **1980**, 344-346.
124. A. S. C. Chan; J. Halpern *J. Am. Chem. Soc.* **1980**, 102, 838-840.
125. B. D. Vineyard; W. S. Knowles; M. J. Sabacky; G. L. Bachman; D. J. Weinkauff *J. Am. Chem. Soc.* **1977**, 99, 5946-5952.
126. P. Barbaro; P. S. Pregosin; R. Salzmänn; A. Albinati; R. W. Kunz *Organometallics* **1995**, 14, 5160-5170.
127. D. Seebach; E. Devaquet; A. Ernst; M. Hayakawa; F. N. M. Kühnle; W. B. Schweizer; B. Weber *Helv. Chim. Acta* **1995**, 78, 1636-1650.
128. K. Zhang; A. A. Gonzalez; C. D. Hoff *J. Am. Chem. Soc.* **1989**, 111, 3627-3632.
129. J. M. Brown; P. L. Evans *Tetrahedron* **1988**, 44, 4905-4916.
130. H. C. Brown; G. Zweifel *J. Am. Chem. Soc.* **1961**, 83, 486-487.
131. H. C. Brown; N. R. Ayyangar; G. Zweifel *J. Am. Chem. Soc.* **1964**, 86, 397-403.
132. H. C. Brown; M. C. Desai; P. K. Jadhav *J. Org. Chem.* **1982**, 47, 5065-5069.
133. H. C. Brown; B. Singaram *J. Am. Chem. Soc.* **1984**, 106, 1797-1800.
134. H. C. Brown; U. P. Dhotke *J. Org. Chem.* **1994**, 59, 2365-2369.
135. H. C. Brown; P. K. Jadhav; A. K. Mandal *J. Org. Chem.* **1982**, 47, 5074-5083.
136. S. Masamune; B. M. Kim; J. S. Peterson; T. Sato; S. J. Veenstra; T. Imai *J. Am. Chem. Soc.* **1985**, 107, 4549-4551; 5832.
137. H. C. Brown; P. K. Jadhav In *Asymmetric Synthesis*; J. D. Morrison, Ed.; Academic: Orlando, 1983; Vol. 5, p 1-43.
138. H. C. Brown; P. K. Jadhav; M. C. Desai *Tetrahedron* **1984**, 40, 1325-1332.
139. H. C. Brown; B. Singaram *Acc. Chem. Res.* **1988**, 21, 287-293.
140. H. C. Brown; J. V. N. V. Prasad *J. Am. Chem. Soc.* **1986**, 108, 2049-2054.
141. K. N. Houk; N. G. Rondan; Y.-D. Wu; J. T. Metz; M. N. Paddon-Row *Tetrahedron* **1984**, 40, 2257-2274.